Universitat de les Illes Balears

BACHELOR'S THESIS

EFFECTS OF MIR-222 ON METABOLIC PROGRAMMING IN OBESITY - IMPACT ON INSULIN SIGNALLING PATHWAY

Pere Bibiloni Coll

Degree in Biochemistry

Faculty of Sciences

Academic Year 2019-20

EFFECTS OF MIR-222 ON METABOLIC PROGRAMMING IN OBESITY - IMPACT ON INSULIN SIGNALLING PATHWAY

Pere Bibiloni Coll

Bachelor's Thesis

Faculty of Sciences

University of the Balearic Islands

Academic Year 2019-20

Key words:

microRNA, insulin signalling pathway, obesity, insulin resistance, adipocytes

Thesis Supervisor's Name: Joana Sànchez Roig

Tutor's Name (if applicable)

Index

Abstract

Obesity is a multifactorial disease of worldwide high-prevalence. The mechanisms behind it are still not completely elucidated. This pathology is usually correlated with insulin resistance, an impaired response to the hormone in peripheral tissues. Some microRNAs, non-coding RNA of around 22 nucleotides with a repression action on other transcripts, are increased in animals or humans with obesity. One of particular interest is miR222, which is believed to have an impact on insulin signalling pathway. However, its exact effects remain unclear. The levels of miR222 were increased in milk from nursing dams fed with a cafeteria diet during lactation, an important period for metabolic programming. Considering this, the aim of this study was to determine the impact of miR222 on insulin signalling route and whether it is transient or permanent, exerting a metabolic programming. To achieve this, transfection with a mimetic (mim222) or an inhibitor (inh222) of the native molecule was performed on a 3T3-L1 *in vitro* model. Both preadipocytes and mature adipocytes were collected to see potential long-term effects. Microarray was conducted to analyse global expression patterns, while RT-qPCR was used to study mRNA levels of selected genes related to the insulin pathway. Protein levels were determined with Western Blotting. Finally, lipid content was quantified utilising Oil-Red staining. Results suggest miR222 has a negative impact on various effectors of the insulin signalling pathway, including *Insr, Irs1* or *Cd36.* Down-regulation of these particular genes has been linked to impaired insulin action in animals and humans. Herein, metabolic programming was not observed as changes in genes studied were generally not preserved. In conclusion, the present work shows that miR222 may play an important role in the disruption of the insulin signalling pathway during obesity.

Resum

L'obesitat és una malaltia multifactorial d'elevada prevalença mundial. Els mecanismes causals encara no estan del tot elucidats. La resistència a la insulina, una resposta inadequada a l'hormona a teixits perifèrics, és una complicació comú en individus obesos. Alguns microARNs, ARN no codificants d'uns 22 nucleòtids de longitud que inhibeixen l'expressió d'altres gens, veuen els seus nivells incrementats en animals i humans amb obesitat. Un d'aquests en concret, el miR222, té un especial interès perquè es creu que podria afectar la via de senyalització de la insulina. Tot i així, els seus efectes concrets encara no han estat determinats. A més, els seus nivells són majors durant la lactància en rates alimentades amb una dieta rica en greixos i sucres (de cafeteria), un període en què es pot exercir una programació metabòlica. Considerant això, l'objectiu del present estudi és determinar l'impacte concret del miR222 sobre la via de senyalització de la insulina i comprovar si pot ser permanent, confirmant així un efecte de programació metabòlica. Amb aquesta finalitat, es dugué a terme una transfecció amb un mimètic (mim222) i un inhibidor (inh222) de la molècula nativa en cèl·lules 3T3-L1, un model *in vitro* d'adipòcits. Per a estudiar l'impacte a llarg termini, es van recollir tant els preadipòcits com els adipòcits madurs. Es realitzà un microarray per estudiar els patrons d'expressió globals, mentre que es dugueren a terme RT-qPCRs per a determinar els canvis concrets de gens d'interès relacionats amb la ruta de la insulina. L'estudi dels nivells de proteïnes d'interès es realitzà amb la tècnica de Western Blotting. Finalment, també s'analitzà el contingut lipídic usant la tinció Oil-Red. Els resultats suggereixen que el miR222 té un impacte en la via de senyalització de la insulina inhibint l'expressió de diversos efectors. Alguns dels més destacats són *Insr, Irs1* o *Cd36*. S'ha vist que la regulació a la baixa d'aquests, tant en models animals com en humans, es correlaciona amb la resistència a la insulina. L'efecte de programació metabòlica no ha pogut ser confirmat ja que la majoria de canvis observats en els gens no es conserven al llarg del temps. En conclusió, aquest estudi demostra que el miR222 pot tenir un paper important en la disrupció de la via de senyalització de la insulina en individus obesos.

Introduction

Obesity and insulin resistance

Obesity is defined as an increased body weight due to abnormal or excessive fat accumulation that may impair health (1,2). It is considered a worldwide health problem, as 13 % of the world's adult population were obese in 2016, tripling the prevalence of 1975. Globally, this disease causes more deaths than undernutrition (1). Both environmental and genetic factors are implied in the onset of obesity (2). Mainly, reduction of physical activity and higher energy intake are responsible of the rise of this epidemic (1,2). Mutations or variations in genes related to energy balance can also increment the susceptibility to its appearance or cause it directly (2). Additionally, this phenotype can be transmitted to future generations due to metabolic programming phenomena during, for example, gestation. Epigenetic alterations are responsible of these long-term gene expression changes (3).

One of the main complications of obesity is the metabolic syndrome (4,5). This disease is characterised by central obesity plus at least two of the following symptoms: raised triglycerides, reduced HDL-cholesterol, raised blood pressure or raised fasting plasma glucose (5). As a whole, this profile is likely to provoke insulin resistance (IR) (4,6).

Insulin is a peptide hormone synthesised by β cells in the pancreas (4,6). Its action is performed in most tissues and its most important effect is to regulate nutrient metabolism, with an important focus on glucose. Briefly, it inhibits gluconeogenesis and stimulates glycogen synthesis at hepatic level; it triggers glucose uptake and utilisation in skeletal muscle and adipose tissue; and upregulates lipogenesis in the latter. By doing this, insulin helps maintaining normoglycemia after ingest of food (4).

In a scenario with IR, insulin-sensitive tissues (liver, adipose tissue and skeletal muscle) present an inadequate response to the hormone (4,6). Insulin signalling pathway is blocked mainly due to modifications in downstream effectors (see next section) (6). Obesity-associated low-grade inflammation may lead to this. Excessive triglycerides stored within the adipose tissue causes cell hypertrophy and an imbalance of adipokine secretory patterns leading towards a pro-inflammatory character. These cytokines impair insulin signalling not only in the adipose tissue but also at a systemic level (4). Mitochondrial dysfunction and endoplasmic reticulum stress are also believed to play an important role in the molecular mechanisms of IR (6).

To compensate this situation, insulin production is increased. Normoglycemia is achieved initially, although this overproduction ultimately leads to pancreatic β cell failure, together with impaired insulin synthesis (4,6). Therefore, IR plays an important role in the pathogenesis of type 2 diabetes (T2D) (6). The impaired function of insulin is the link between obesity and T2D, which is a common complication in obese individuals (4,6).

Molecular mechanisms of insulin signalling pathway

The insulin signalling pathway (**Figure 1**) is initialised by the attachment of the hormone to the insulin receptor (INSR). This induces the autophosphorylation action of the transmembrane receptor on tyrosine residues. Insulin receptor substrate (IRS) has affinity for these modifications and is also a substrate for the tyrosine phosphorylation activity. Afterwards, it recruits phosphatidylinositol-3-kinase (PI3K). This protein catalyses the phosphorylation of phosphatidylinositol-4,5-biphosphate (PIP2) – a plasma membrane component – to phosphatidylinositol-3,4,5-triphosphate (PIP3). Phosphoinositide-

dependent kinase (PDK) is recruited next and activates protein kinase B (PKB or AKT), which plays a central role in the transduction of the signal (6,7). Several substrates are susceptible of its action:

- Vesicles which contain glucose transporter 4 (GLUT4) are kept in the cytoplasm due to the action of TBC domain family member 4 (TBC1D4). AKT represses the action of this protein, allowing the fusion of the vesicles to the membrane and hence the glucose uptake (6,7).
- Forkhead family box O (FOXO) phosphorylation causes its nuclear exclusion and posterior degradation. This transcription factor promotes the output of glucose and inhibits glycolysis. Thus, insulin signalling provokes glucose utilisation (6,7).
- Phosphorylation of glycogen synthase kinase 3β (GSK3β) stops its activity. Consequently, synthesis of glycogen is activated. This is particularly important in the liver (6,7).
- The protein tuberous sclerosis 2 (TSC2) is also inhibited by AKT, which allows activation of mechanistic target of rapamycin complex 1 (mTORC1) and its downstream targets: ribosomal protein S6 kinase (S6K) and sterol regulatory element binging protein 1c (SREBP1c). The former provokes an increase of protein synthesis, while the latter triggers lipogenesis (6,7).

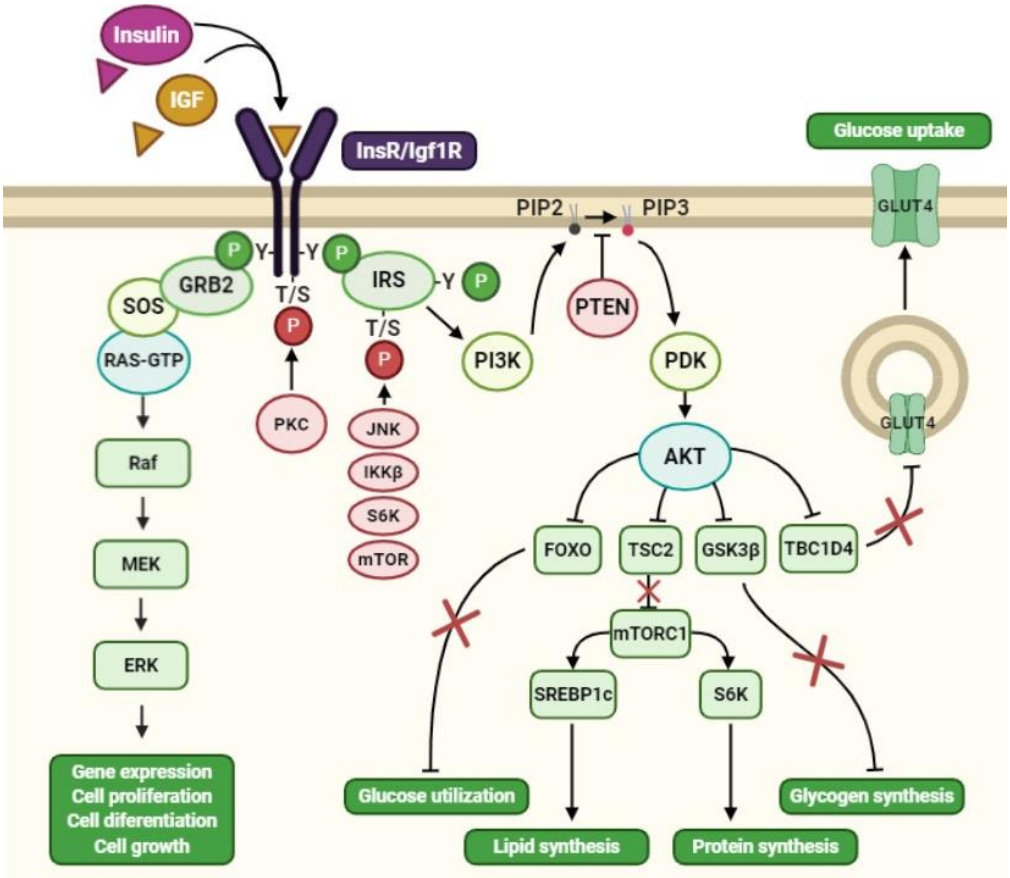

Figure 1. *Insulin signalling pathway. Green/blue: effectors of the route. Red: antagonists. S: serine. T: threonine. Y: tyrosine. Image generated with Biorender.com and adapted from* (6,7).

An alternative pathway to PI3K/AKT involves the activation of MAP kinases that regulate gene expression, cell proliferation, cell differentiation and cell growth (6). This route is more relevant for insulin-like growth factor (IGF), an insulin analogue that interacts with IGF receptor (IGF1R). Both ligands and receptors show a high homology, reason why their signalling pathways exhibit common effectors and cross-reactivity (8). Overall, insulin signalling system can be classified as anabolic.

Regulation of the insulin signalling pathway occurs through different mechanisms, such as negative effectors that diminish the activation of the proteins involved (6,7). On one hand, these can act as phosphatases, such as PTEN, which reverts the action of PI3K. Its insufficient expression or action results in increased insulin sensitivity. On the other hand, we find inhibitory phosphorylation. This can be performed on both INSR and IRS and, contrary to the activation, kinases act on serine or threonine residues. This type of repression usually triggers IR in obesity. Lipotoxicity caused by the increment of lipid accumulation activates the PKC that inhibits INSR. Inflammatory cytokines such as tumour necrosis factor α (TNFα), interleukine 6 (IL-6) or interleukine 1β (IL-1β), increased in obesity, promote the activation of several serine/threonine kinases that act on IRS. Most representative examples are c-Jun N-terminal kinase (JNK); IκB kinase β (IKKβ), S6K and mTOR (7). Moreover, genetic expression of the components of the pathway can be altered as another way of regulation or to contribute to the appearance of IR. For instance, it is common that insulin-resistant cells present lower levels of INSR in their membranes compared to wild-type cells (6).

MicroRNAs: biogenesis, mechanism of action and biological function

MicroRNAs (miRNAs) are non-coding RNA of approximately 22 nucleotides (nt) long. They participate in the posttranscriptional regulation of gene expression. Mainly, miRNAs silence messenger RNA (mRNA) targets by direct attachment. miRNAs were discovered in 1993 in *Caenorhabditis elegans* non-vertebrate animal model, but soon after they were found in evolutively higher species – including humans. A great number of these molecules are highly conserved in animals, which proves the important role they play (9,10).

In the predominant biogenesis pathway (**Figure 2**), miRNAs are firstly transcribed by RNA polymerase II (RNA pol II) in a primary form (pri-miRNA). One or more regions of their structure fold back on themselves to form a hairpin structure. Then, the heterotrimer microprocessor, formed by the endonuclease Drosha plus two regulatory components, interacts with these newly formed estructures. Drosha subunit undergoes double strand cuts on one end of the pri-miRNAs, releasing 60 nt stem-loop structures called pre-miRNAs. At this point, pre-miRNAs are exported to the cytoplasm by the exportin 5 in a RAN-GTP dependent way. DICER, another endonuclease, cuts the double strand close to the loop. The result includes the final miRNA and a passenger strand (miRNA*). Finally, the miRNA duplex is loaded on an Argonaute protein (AGO), which then expulses the miRNA* - that is degradated - and forms the silencing complex. This complex will interact with mRNAs to regulate their expression (9,10).

Other non-canonical biogenesis pathways have been described, such as miRNAs derived from introns. They are synthesised during splicing of other genes. Regardless the route of biogenesis followed, the final silencing complex is equally generated and performs the repression function (9).

The target recognition is usually done through a direct interaction between the seed sequence at the 5' end of the miRNA and the 3' untranslated region (3' UTR) of the target mRNA (9,10). Nevertheless, miRNA can be paired to other sites as well, such as 5' UTR or the open reading frame (ORF) itself. The silencing of the target gene following this annealing can be performed through different mechanisms. In superior animals, the dominant mode consists in the recruitment of adaptor proteins by AGO protein. This complex itself can difficult translation of the transcript. It can also recruit deadenylases complexes, which shorten the mRNA poly(A) tail. This destabilises the mRNA and, in consequence, triggers its degradation (9).

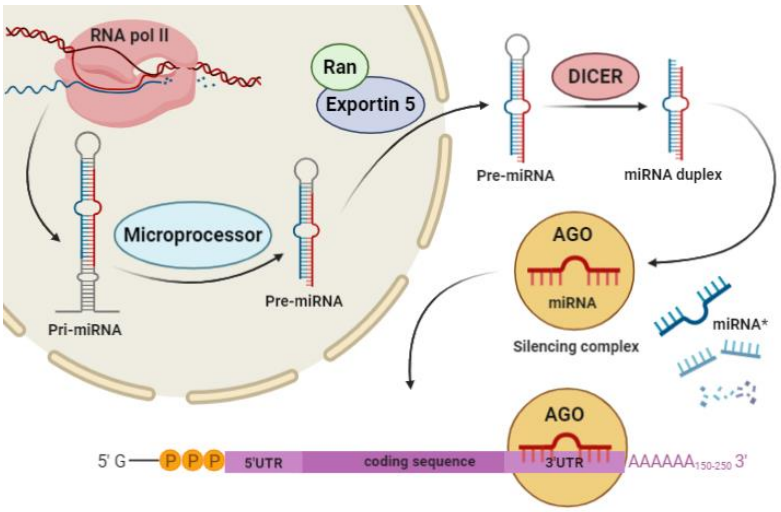

Figure 2. *Canonical pathway of miRNAs biogenesis. Image generated with Biorender.com and adapted from* (9).

As a whole, miRNAs act as an additional layer of posttranscriptional gene control and, therefore, are considered an epigenetic mechanism. The repression caused is often discrete, among 20 % or 50 %, which permits adjusting protein expression to specific and optimal levels needed (9,11). Plus, they participate in many conserved pathways: in human genome, an estimated 60 % of genes are controlled by miRNAs (10). The short length of seed sequences allows a single miRNA to regulate dozens or hundreds of genes (12). In consequence, miRNAs are placed in a privileged position when it comes to regulate complex networks in order to cope with environmental changes (9).

MicroRNAs role in diseases: miR222 in obesity and insulin resistance

Different pools of miRNA are found in different cell types at several developmental stages (9) and "they define the physiological nature of the cell" (12). Specifically, several miRNA play essential roles in biological functions such as intracellular signalling or cellular metabolism. Consequently, aberrant expression of these molecules can lead to cell malfunction and, ultimately, to disease (12). This was confirmed with several studies that showed aberrant miRNA expression patterns for concrete pathologies and processes. Some examples are ageing, cancer, cardiovascular diseases, autoimmune diseases, infections and neurodegenerative diseases (11,12). Furthermore, the tissue deregulation is mirrored in blood circulation. As a result, miRNA may be used to improve prognosis of diseases (13). They are thought to be "top candidate for the next generation of biomarkers" (12). Interventions based on their alteration are also being studied (11,12).

Obesity and metabolic disease have been related to dysregulated miRNA expression patterns (10,13). For instance: miR-17/92 family, the miR-143-145 cluster, miR130 family and let-7 family, among others (10). One miRNA of particular interest is miR222. It "shows arguably the greatest promise as a clinical biomarker of metabolic disease" (10).

In animal models, obesity or related conditions are linked to an elevation of miR222 expression levels in adipose tissue. In mice with obesity induced by a long-term high-fat diet, adipose tissue exhibited higher miR222 concentrations than wild-type group (14). Spontaneous T2D rat model presented upregulated miR222 in the adipose tissue, whereas it did not present any changes in other tissues targeted by insulin (15).

Similar results were obtained in human studies. Ortega et al. (13) showed that miR222 circulating levels were significantly higher in humans with morbid obesity. In another study, their levels in serum were greatly increased in obese children when compared to healthy subjects (>6-fold) (16). A different research reported elevated miR222 levels in men with T2D, both obese and non obese. Interestingly, this rise was not observed in obese individuals who presented normal glucose tolerance. Moreover, metformin, an insulin sensitizer drug used to treat T2D, decreased the increment of miR222 (17).

Altogether, these results suggest that, within the broad obesity phenotype, miR222 is particularly involved in the insulin signalling pathway in white adipose tissue. It may have a role in the development of insulin resistance (10). Several miR222 targets have been established in 3T3-L1 adipocytes. Oestrogen receptor α (ERα) expression was significantly decreased when cells were exposed to miR222, alongside with GLUT4 (18). Adiponectin receptor 1 (ADIPOR1) - with a protective role on insulin resistance and obesity – and B-cell translocation gene 2 (BTG2) – a cell proliferation inhibitor – were downregulated when exposed to a miR222 analogue (19). In other cell lines, direct effectors of insulin have been established as targets of this miRNA: IRS1 in liver cells (20) and PTEN in breast cancer cells (21). However, effects of miR222 in insulin signalling route on adipocytes remain unclear.

Furthermore, in a recent study (22), it was shown that cafeteria diet (rich in carbohydrates and lipids) during lactation altered miR222 levels in milk (among other miRNAs). The offspring of these dams developed an obese phenotype in adulthood: they had greater fat accumulation and presented an altered insulin signalling (impaired response to an oral glucose tolerance test). It is considered that milk can act as a vehicle to transfer miRNAs to offspring, which would incorporate them. Thus, it may be speculated from these results that miR222 could be responsible for the long-terms changes in insulin signalling pathway. Epigenetic changes occurred during early life stages would persist until adulthood – miR222 would be able to exert metabolic programming effects (22). Molecular mechanisms underneath these observations are not completely understood yet.

Objectives and experimental design

It is known that miR222 is related to obesity and IR. Evidence suggests that it may exert its effects through modification of the insulin signalling pathway, specifically in adipocytes. In addition, miR222 levels increase in milk during cafeteria diet. Lactation is an important period for metabolic programming and phenotype changes in offspring's adulthood are a proof for this. Therefore, it was hypothesised that increased levels of miR222 may be responsible of changes in insulin signalling pathway in adipocytes, which may be permanent and cause metabolic programming effects. This would lead to a high susceptibility to obesity and/or insulin resistance in the future.

Taking everything into account, the aim of this project is to determine the effects of miR222 on insulin signalling pathway in adipocytes. The metabolic programming that this may cause is also an aim of study. To achieve this, 3T3-L1 adipocytes, an *in vitro* cell line from *Mus musculus,* were used. Transfection of a miR222 mimetic was conducted to emulate the exposure to the native molecule and validate their target genes. In addition, an inhibitor of miR222 was utilised to better comprehend the impact of the microRNA. In order to study possible long-term effects of the treatment, two stages of cell differentiation were studied: preadipocytes and mature adipocytes.

Effects on gene expression were studied at transcriptional and translational levels. Microarrays were performed to analyse global mRNA expression, while retrotranscriptase-quantitative polymerase chain

reaction (RT-qPCR) was carried out to study expression of selected genes of interest. Protein expression was examined through Western Blotting. Finally, total lipid content was determined as a final consequence of alterations in the adipocyte metabolism.

This project was undertaken as the Final Degree Thesis of the author. Part of the presented results were obtained in the frame of a Collaborating Student Scholarship granted by the "*Ministerio de Educación y Formación Profesional*" during the 2019/2020 academic year. This work also takes part in the project "PI17/01614", funded by "*Instituto de Salud Carlos III"* and cofounded by European Union (ERDF/ESF, "Investing in your future").

Materials and methods

Cell culture and transfection

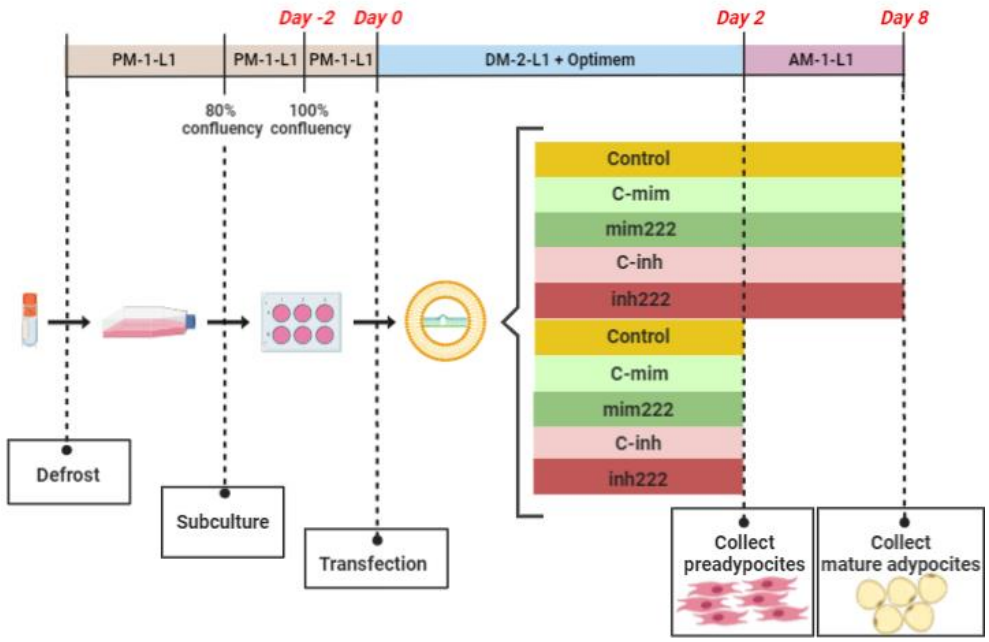

Figure 3. *Experimental design of cell culture. Image generated with Biorender.com*

The experimental design is schematised in **Figure 3**. 3T3-L1 preadipocytes at passage number 10 were used. Cryovials were defrosted and resuspended with preadipocyte medium (PM-1-L1). Manual cell counting of the resulting solution was conducted using a Neubauer chamber in a Tripan blue solution 1:1. Four visual camps were analysed and the average was calculated. The initial pool of cells was distributed into 75 cm^2 flasks taking into account their maximum capacity - 100.000 cells per flask. The resulting culture was incubated until 70-80 % confluency at 10 % CO_2 and 37 ºC. Culture medium was changed every two days.

After that condition was reached (4 days approximately), cells were subcultured (passage number 11). Acutase was utilised in order to detach the cells. Cells were counted using the same procedure described above. The solution was divided in 6-wells plates with 38.000 cells per well. PM-1-L1 medium was still used and changed every two days. Same incubation conditions were assured until 100 % confluency (day -2).

Forty-eight hours upon confluency completion (day 0), transfection was performed using OptiMEM and lipofectamine according to the manufacturer's protocol. Differentiation medium (DM-2-L1) was used to induce cell differentiation. Cells were divided into different groups depending on the RNA transfected:

- **Control (C)**: No RNA transfected
- **Mimetic negative control (C-mim)**: No known effect double strand RNA with random sequence
- **miR222 mimetic (mim222)**: Double strand RNA with miR222 sequence
- **Inhibitor negative control (C-inh)**: No known effect single strand RNA, random sequence
- **miR222 inhibitor (inh222)**: Single strand RNA with a complementary sequence to miR222

Cells were incubated at 8 % CO_2 and 37 ºC. At day 2 (48h after transfection), half of the plates were collected – the medium was extracted and they were stored at -80 ºC (*preadipocytes*). The rest were incubated 6 days more in order to permit their final differentiation into adipocytes (*mature adipocytes*). In these plates, culture medium was changed to adipocyte maintenance medium (AM-1-L1) from this point on, while incubation conditions were not altered. Medium change was performed every two days. Simultaneously, pictures were taken using an optical microscope to study the differentiation progress. Upon differentiation completion, plates were collected (day 8).

The same procedure was repeated three times for different analyses, including RNA expression through RT-qPCR, transcriptomic analysis with a microarray and western blotting. Experimental groups and number of samples per group were adjusted in each case to specific purposes (**Table 1**).

Table 1. *Number of samples for each experimental group and analysis. WB: Western blotting*

Experiment	**Preadipocytes**					**Mature adipocytes**				
Group	**C**	**C-mim**	**mim222**	**C-inh**	**inh222**	**C**	**C-mim**	**mim222**	**C-inh**	**inh222**
Microarray	4	4	4	-	-	4	4	4	-	-
RT-qPCR	10	7	10	4	5	10	7	10	4	5
WB	13	7	7	6	6	7	7	7	-	-
Oil-Red	-	-	-	-	-	7	7	10	-	-

The author of this thesis collaborated in the realisation of the cell culture for the protein analysis, while the other ones were performed previously.

Analysis of mRNA levels of genes of interest

Target genes selection

Genes directly involved in the insulin signalling pathway were chosen, according to Wiki pathways (23). From all the downstream possibilities, special emphasis was put on genes related to lipid metabolism. Then, miRDB online database (24) was checked to search for predicted miR222 target genes involved in this pathway. Among them, *Igf2bp2* was selected as a predicted miR222 target gene with a target score of 61. Furthermore, a previously validated miR222 target gene, *Cdkn1b* (25), was included to contrast results. This work's author collaborated in the gene research, although most of the genes were chosen according to its primers availability in the laboratory.

RNA extraction and RT-qPCR

RNA was extracted using TriReagent protocol instructions. Samples were quantified with Nanodrop, making sure A260/A280 and A260/A230 ratios were optimal. Dilutions were prepared to a 25 ng/µL

final concentration. RT was performed using iScript cDNA Synthesis kit according to protocol's guidelines. 1/10 dilution of the product was used to perform qPCR with SyBrGreen-mix. Primers used are described in **Table 2**. qPCR was carried out in StepOne Plus Real-Time PCR System.

Table 2. *Genes analysed. Primers used in qPCR, both forward and reverse respectively. Primers for genes underlined were specifically designed by the author of this thesis for this project purpose.*

Gene ID	Product name	Primers sequence (5'→3')
Actb	β-Actin	TACAGCTTCACCACCACAGC TCTCCAGGGAGGAAGAGGAT
Akt1	Protein kinase B	TAGGCCCAGTCGCCCG AGGTGCCATCGTTCTTGAGG
Cd36	Cluster of differentiation 36	GTGGCAAAGAACAGCAGCAA CCAACAGACAGTGAAGGCTCA
Cdkn1b	Cyclin-dependent kinase inhibitor 1B	CAGAATCATAAGCCCCTGGA GACGAGTCAGGCATTTGGTC
Cpt1b	Carnitine palmitoyltransferase 1B	AAGGGTAGAGTGGGCAGAGG GCAGGAGATAAGGGTGAAAGA
Fasn	Fatty acid synthase	TTCGGTGTATCCTGCTGTCC TGGGCTTGTCCTGCTCTAAC
Gdi1	Guanosine nucleotide dissociation inhibitor 1	CCGCACAAGGCAAATACATC GACTCTCTGAACCGTCATCAA
Igf1	Insulin-like growth factor 1	GCTGGTGGATGCTCTTCA CGATAGGGACGGGGACTT
Igf1r	Insulin-like growth factor 1 receptor	CACAACTACTGCTCCAAAGACAA CGTCTCTCCGCCTCCTTTC
Igf2bp2	Insulin-like growth factor 2 mRNA-binding protein 2	TCCTTCACCCCCTCATCGT TGTCCCTTCTGGGGTAGCAT
Insig1	Insulin-induced gene 1 protein	AGCGTTATGCGCTGTATTGC AGGCGATGGTAATCCCAAGC
Insr	Insulin receptor	TGGAGAGGTGTGCCCTGGTA ATCTTCGGGTCTGGTCTTGAAC
Irs1	Insulin receptor substrate 1	TGGAGTATTATGAGAACGAGAAGA CCCGCTTGTTGATGTTGAAA
Lipe	Hormone-sensitive lipase	TCACGCTACATAAAGGCTGCT CCACCCGTAAAGAGGGAACT
Lpl	Lipoprotein lipase	TTCAACCACAGCAGCAAGAC CCACATCATTTCCCACCAG
Pik3r1	Phosphatidylinositol 3-kinase regulatory subunit alpha	AGCTGGATGTGAAGTTGCTCT TCCTGGGTTTGGCATTGTTCT
Pparγ	Peroxisome proliferator-activated receptor gamma	AGACCACTCGCATTCCTTTG TCGCACTTTGGTATTCTTGG
Prkaa1	5'-AMP-activated protein kinase catalytic subunit alpha-1	AGGCACCCTCACATCATCAA ACCACCATATGCCTGTGACA
Pten	Phosphatase and tensin homolog	CAAGGAGTATCTTGTACTCACCC GCCTCTGGATTTGATGGCTC
Scl2a4	Glucose transporter type 4	GCCATCTTCTCTGTGGGTGG GAAGATGAGTGGGGGCGATT
Srebf1	Sterol regulatory element-binding protein	CAGCGGTTTTGAACGACA GCCAGAGAAGCAGAAGAGAAG

StepOne Plus Software v2.2.2 was used to process results. Samples with different melting curves or/and abnormal amplification plots were discarded. Crossing points (C_P) of the remaining were used to calculate their expression standardized by the housekeeping gene using the $2^{-\Delta\Delta CP}$ method. Control levels from preadipocytes were taken as 100 % and the other groups were expressed as the relative expression in comparison.

The housekeeping gene was chosen among GDI and β-actin analysing the statistical parameters of their C_P. ANOVA showed differences between groups in both cellular states for β-actin, while no variations were observed among groups in preadipocytes for GDI. From these results, GDI was selected for all the required calculations.

RNA extraction was performed before the beginning of this project. The scholar carried out the remaining tasks from that point on.

Primers design

The lab already owned most of primers used in RT-qPCR. Other primers for genes of interest (*Igf2bp2, Pten, Akt1, Pik3r1, Slc2a4* and *Igfr1*) were designed using Primer-Blast tool from the National Center for Biotechnology Information (NCBI). The parameters established were amplicon size of 100-250 bp, intron inclusion and melting temperature of 57.0-63.5 ºC. From the results displayed, primers with best scores were chosen and ordered.

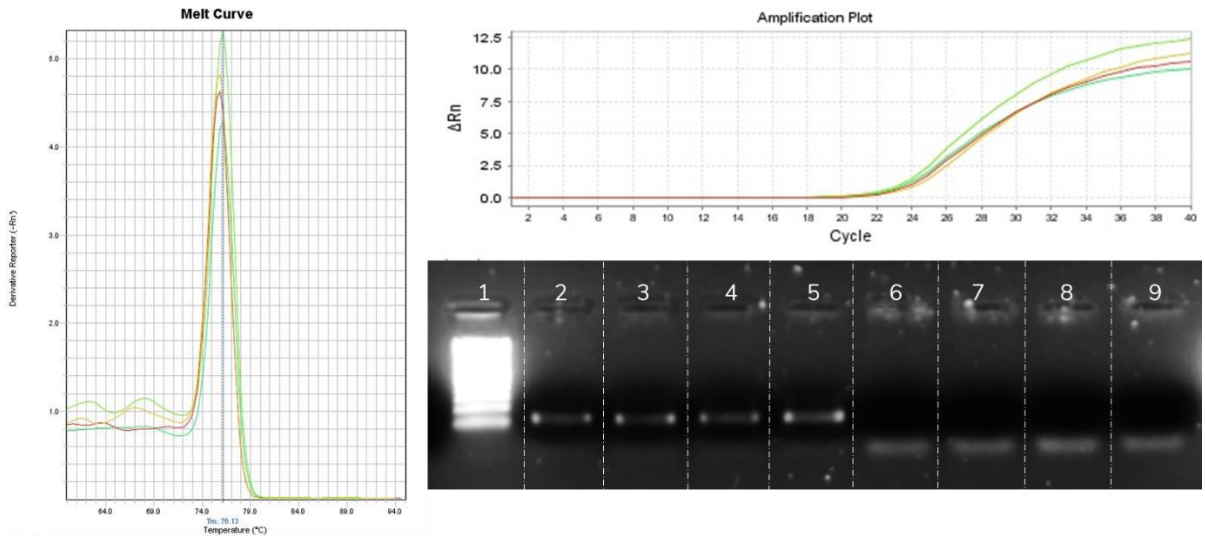

Figure 4. *qPCR results of four samples using PTEN designed primers. Left: melting curve plot. Right top: amplification plot. Right bottom: electrophoresis result. 1st lane: molecular weight ladder. 2nd and 3rd lanes: preadipocytes control. 4th and 5th lanes: matures adipocytes control. 6th and 7th lanes: RT blank. 8th and 9th lanes: PCR blank.*

Once received, a test was undertaken in order to assure their specificity. qPCR was performed using cDNA from control samples and the new primers. One melting curve and similar C_P's between samples were observed for each primer (**Figure 4**, left and right top). The amplification product was loaded in a 2 % w/v agarose gel with SYBR safe. iBright CL750 Imaging System (Thermofisher) was used for visualization. Images showed a unique band with a molecular weight similar to the expected and no amplification for RT and PCR blanks. For example, in the case of PTEN only a band between 100 bp

and 200 bp was shown, agreeing to the expected 141 bp (**Figure 4**, right bottom). Regarding these results, primers were considered successfully designed.

The author of this thesis undertook both the primer design and the primer verification.

Microarray experiment

RNA was extracted using TriReagent protocol instructions. From this point on, procedure was carried out by an external group: "Servicio de Genómica y Genética Traslacional" from the "Centro de Investigación Príncipe Felipe".

Quality of the samples was assured with a RNA intregrity number (RIN) superior than 9. This control was performed on Agilent 2100 Byoanalyzer with RNA 6000 Nano chips (Agilent Technologies, Barcelona, Spain). Microarray processing was done using Mouse GE 8x60K Microarray according to manufacturer's protocol (Agilent Technologies).

Raw data background was corrected following the Agilent methodology continuing with its standardization by quantile normalisation. Differences in expression were calculated with moderate t-statistic of the Limma package and adjusting the p-values using Benjamini-Hochberg method. In addition, an analysis of signalling routes with Hipathia was performed. Contrast is done with Limma to compare the activation levels of each sub-route between two experimental groups of interest, and thus check the route has been activated or inhibited.

The student contributed to the analysis of microarray results included in this Final Degree Project. Concretely, heatmaps were done using data obtained from this technique. R (v 3.3.1. R Development Core Team) and RStudio software were utilised for this purpose.

Protein extraction and Western Blotting

Cell plates were scrapped in RIPA-buffer with proteases and phosphatases inhibitors. The resulting cell solution was further homogenised using a Polytron homogenizer. The protein extract was quantified with bicinchoninic acid assay (BCA) following the manufacturer's instructions. Twenty micrograms of protein were loaded into precast electrophoresis gels with sample buffer in a 1:4 proportion. Following 1.5 h of electrophoresis run, proteins were transferred to a membrane using Trans-Blot Turbo Transfer System. One hour incubation with blocking buffer preceded incubation with primary antibodies overnight (Cell Signalling Technology) targeting proteins whose genes were studied with RT-qPCR (**Table 3**). Membranes were washed out with a mixture of tris-buffered saline and Tween (TBST). Next, secondary antibodies against mouse or rabbit were used depending on the primary antibody source. Before images were taken, several washes using both TBST and tris-buffered saline (TBS) were performed. Fluorescence was visualised with Odyssey (LI-COR) at 700 nm or 800 nm (anti-mouse or anti-rabbit, respectively). Stripping was performed between lectures to detach secondary antibodies and allow new probes. Target proteins with similar molecular weight and same antibody source (e.g. AKT and AMPK1a) were studied in different gels to avoid possible interferences.

Odyssey V3.0 software was used to analyse bands intensity. Lanes and bands were manually selected and background was automatically corrected using *lane background* method. Three samples were repeatedly analysed in all gels in order to show possible differences between them. The ratios of these variations were used to correct all intensities. Afterwards, they were standardised with B-ACTIN intensity and expressed as percentage of expression compared to control group, considered 100 %.

The author of this thesis participated actively in all the tasks included in this section.

Table 3. *Target proteins of the primary antibodies used*

Target protein	Target molecular weight (kDa)	Antibody source
INSR	95	Rabbit
AMPK1a	62	Rabbit
AKT	60	Rabbit
PTEN	54	Mouse
β-ACTIN	45	Mouse

Oil-Red staining

Oil-Red staining and further quantification was performed to study lipid content. Mature adipocytes were collected and sequentially washed out with: phosphate-buffered saline (PBS), 10 % formaldehyde solution, double distilled water (ddH_2O) and 60 % isopropanol solution. Cells were completely dried and then incubated 10 min with Oil-Red reagent. After staining, samples were washed out again with ddH_2O. At this point, cells were observed under the microscope and pictures were taken. Next, isopropanol was added in order to extract Oil-Red from cells. Optical density from the resulting solutions was measured at 500 nm using a Tecan sunrise microplate reader and 100 % isopropanol solution as blank. Results obtained were expressed as relative lipid content, considering the control group mean as 100 %.

The student collaborated in all the parts of this experimental protocol.

Data processing and statistical analysis

Except for the microarray data, all the parameters mentioned above were processed and statistically analysed in the same way. Microsoft Excel was used to obtain their mean and standard error of the mean (SEM) and represent them graphically. Statistical differences among experimental groups were evaluated by Mann-Whitney U test in IBM SPSS Statistics software. This was the most appropriate method because 1) samples were independent; 2) the majority did not present a normal distribution, therefore requiring a non-parametric test; 3) number of individuals per group (n) was less than 10.

In concrete, the following contrasts were evaluated (if applicable): Control vs C-mim, Control vs mim222, Control vs C-inh, Control vs inh222, C-mim vs mim222 and C-inh vs inh222. Preadipocytes and mature adipocytes were regarded as two independent groups, totalling 12 comparisons.

The statistical analysis workload was performed entirely by the author of this project.

Results

3T3-L1 adipocytes differentiation and morphology monitoring

Transfection with mimetic negative control (C-mim) and miR222 mimetic (mim222) was conducted at day 0 (48 h upon confluence completion) until day 2, when medium was replaced. Half of the wells were collected at day 2 (preadipocytes group), whereas the other half continued the differentiation process until day 8 (mature adipocytes group) (**Figure 3**).

Images were taken from day 2 to day 8, before mature adipocytes were collected. No appreciable differences were found amongst plates. One representative example is shown in **Figure 5**. Photographs demonstrate that initial preadipocytes properly differentiate into mature adipocytes. It can be seen that

spindle-shaped cells transform into round-shaped cells. Fat accumulation can also be observed as white/yellow droplets.

Cell differentiation is present in all experimental groups. This proves that transfection did not prevent the physiological process progression. Even though mim222 group seemed to have greater lipid content at day 4, no significant differences were found in the following days (**Figure 5**).

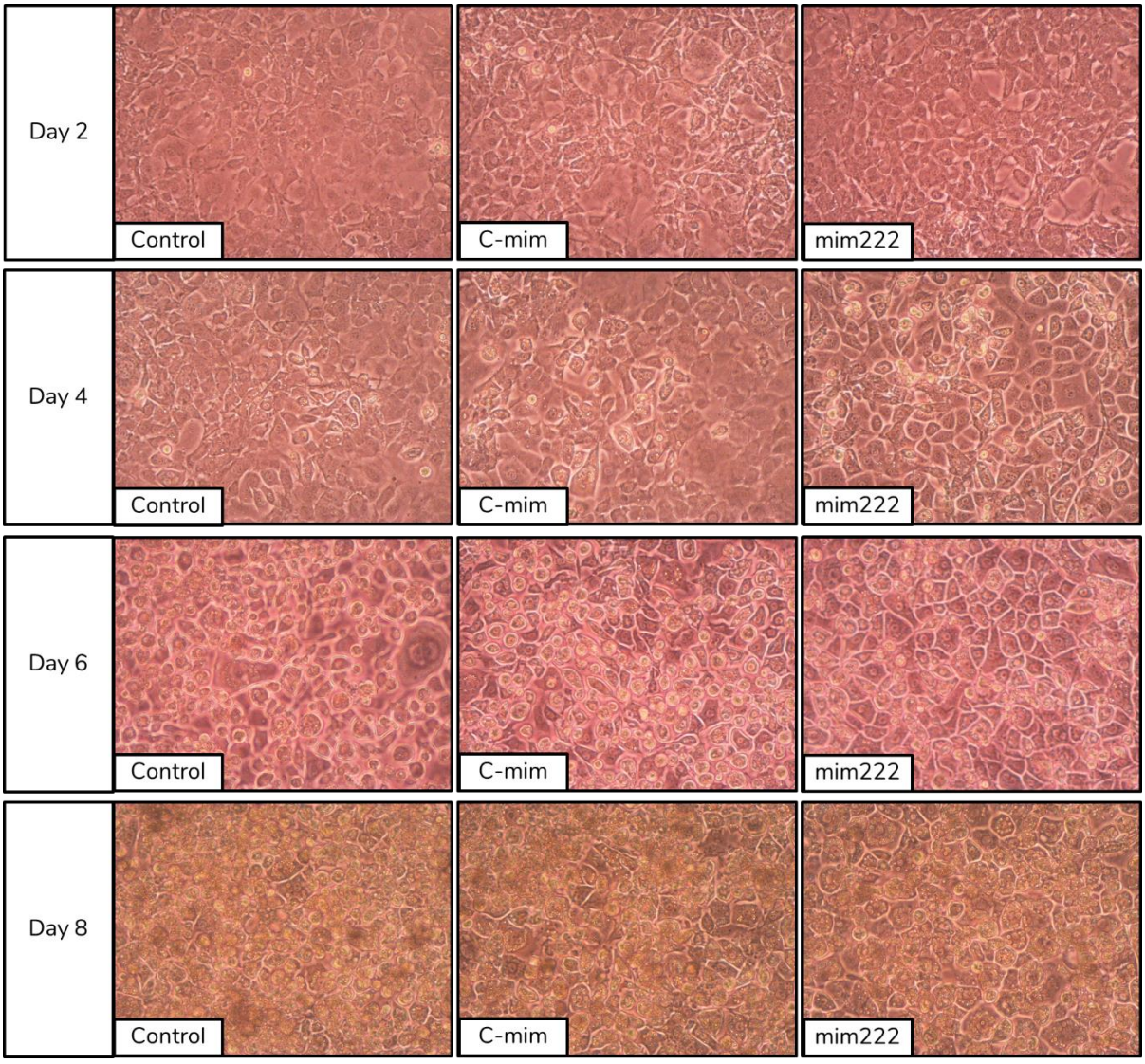

Figure 5. *Evolution of cell differentiation from preadipocytes to mature adipocytes, starting from day 2 (recollection of preadipocytes) until day 8 (just before recollection of mature adipocytes). Photographs were taken to the 3 same wells every day, one of each group: Control, C-mim and mim222. Images were taken with an optical microscope at 10x.*

Lipid content

Images of mature adipocytes were taken after oil-red staining (**Figure 6**). No significant differences can be observed between groups, suggesting that mim222 did not cause an effect in cellular lipid content. This conclusion is supported by quantification results (**Figure 7**). Although it seems that mim222 causes a slight decrease, this difference is not statistically significant. Therefore, it can be concluded that total lipid content was not altered due to mim222 treatment.

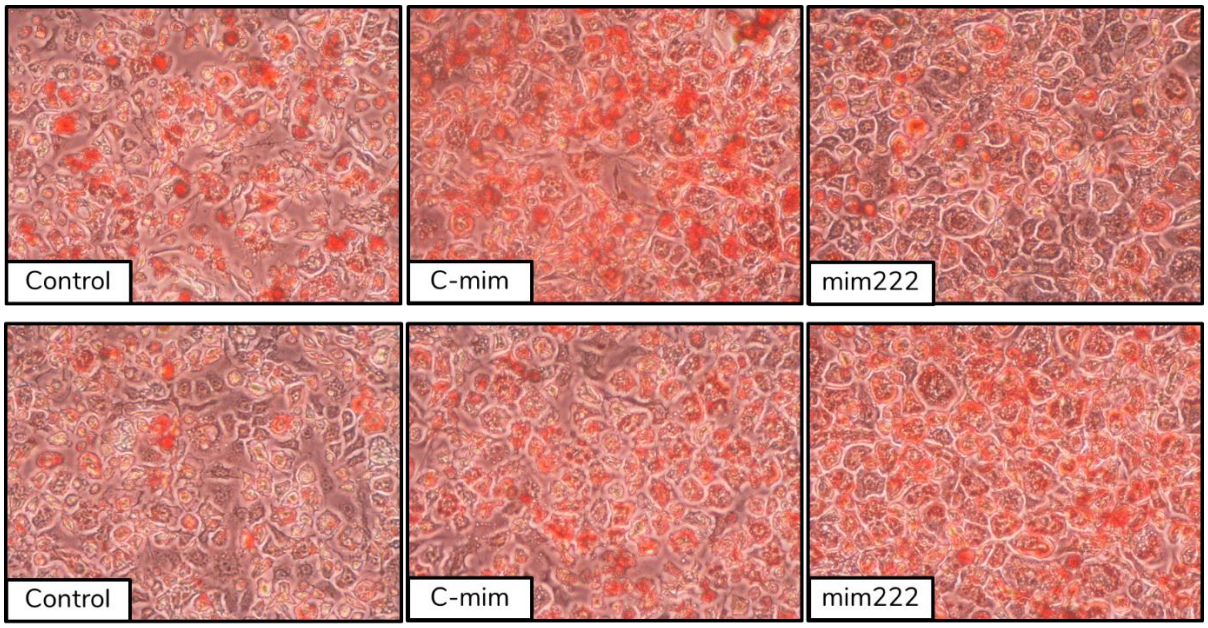

Figure 6. *Oil-Red staining of mature adipocytes. Samples from the same row were in the same plate. Images were taken with an optical microscope at 10x.*

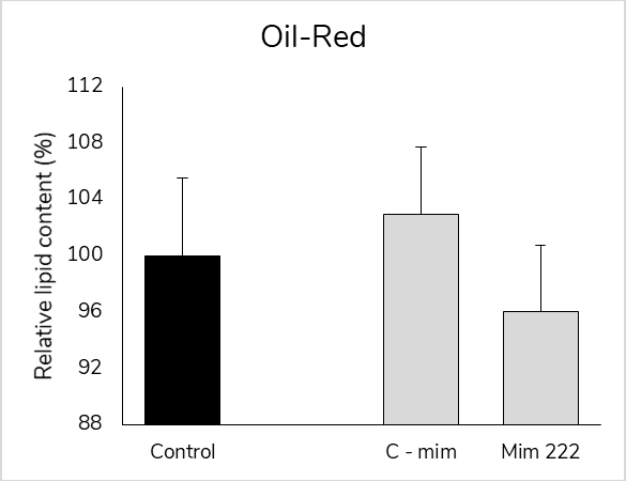

Figure 7. *Levels of lipid content obtained by oil-red technique. Data are mean ± SEM.*

Effect of mim222 on mRNA levels of genes related to insulin signalling pathway

Microarray experiment

A microarray analysis was performed with a subset of samples from selected groups from preadipocytes and mature adipocytes: Control, C-mim and mim222.

Analysis of signalling routes performed shows that 146 pathways were altered with treatment when comparing C-mim and mim222 group. Interestingly, three routes related to insulin signalling pathway were included:

- Insulin signalling pathway: D-Glucose (ID: P-mmu04910-17)
- Central carbon metabolism in cancer: PTEN (ID: P-mmu05230-100)
- PPAR signalling pathway: Aqp7 (ID: P-mmu03320-7)

For all of them, a negative fold change and an adjusted p-value inferior to 0.05 were obtained. These results were observed both in preadipocytes and in mature adipocytes. Hence, an inhibitory effect on insulin signalling pathway due to mim222 is demonstrated. Taking these results into consideration, analysis on single genes related to this route was performed.

Heatmap from microarray data was constructed contemplating only selected genes implied in insulin signalling pathway. The resulting graphic (**Figure 8**) clearly shows two clusters, each representing a different cell stage: preadipocytes and mature adipocytes. This demonstrates that gene expression significantly changes during differentiation and serves as another proof of this process happening. To better observe genes changes depending on experimental treatment, further heatmaps of each cell stage were conducted (**Figure 9**, **Figure 10**).

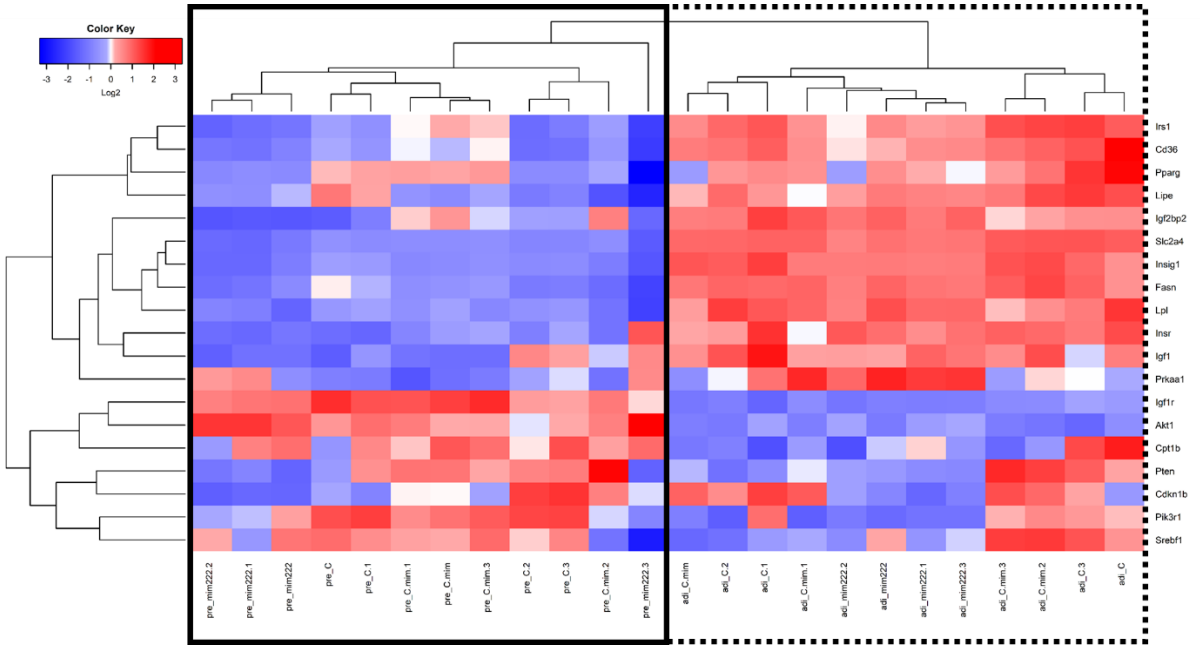

Figure 8. *Heatmap representation of microarray results for genes of interest from all the groups analysed. Clusters are represented for both samples (vertical) and genes (horizontal). Blue: repression. Red: overexpression. Solid-line box: cluster of samples from preadipocytes. Dotted-line box: cluster of samples from adipocytes.*

Heatmap for preadipocytes samples shows that most mim222 group samples are grouped firstly (**Figure 9**, yellow solid-line box). The remaining mim222 sample (number 3) presents a similar gene expression pattern, but more intense, reason why it is clustered in the last instance. Taking into consideration the cluster of genes, two groups can be distinguished. On one hand, the ones that are overexpressed in mim222 samples compared to Control and C-mim samples (**Figure 9**, dotted-line box). On the other hand, genes that are repressed in mim222 treatment samples compared to Control and C-mim groups (**Figure 9**, solid-line box). It can be seen that a greater amount of genes have been repressed with mim222 treatment, which agrees with the theoretical miRNA function.

Mature adipocytes results show a similar trend. In this case, no mim222 outlier sample is found, as all of them form a cluster at first (**Figure 10,** yellow solid-line box). More genes show a decrease in their expression as result of mim222 treatment (**Figure 10,** black solid-line box). Genes with a higher expression (**Figure 10,** black dotted-line box) are a minority in comparison. Two out of these four genes are the same ones overexpressed in preadipocytes: *Akt1* and *Prkaa1*. These results suggest that,

overall, gene expression changes due to experimental treatment are similar in both cell stages. Therefore, it may be inferred that mimic effects are maintained until final differentiation (day 8), even though mimic was only present until day 2.

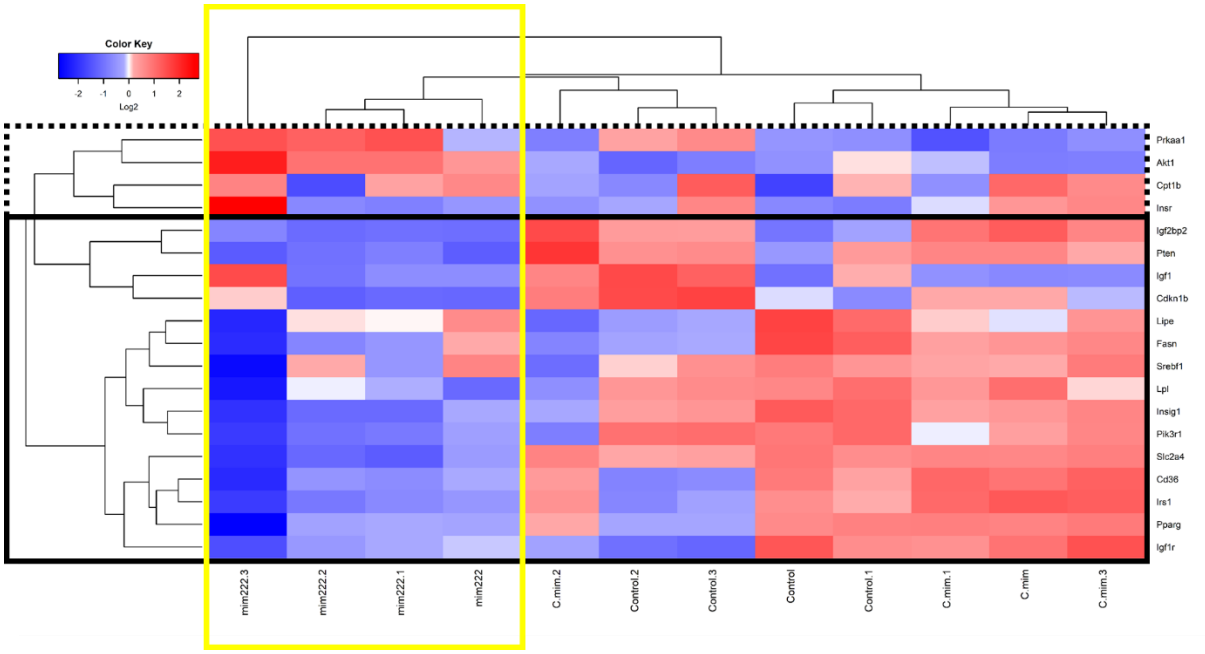

Figure 9. *Heatmap representation of microarray results for genes of interest from preadipocytes samples. Clusters are represented for both samples (vertical) and genes (horizontal). Blue: repression. Red: overexpression. Black solid-line box: cluster of genes repressed with mim222 treatment. Black dotted-line box: cluster of genes overexpressed with mim222 treatment. Yellow solid-line box: cluster of mim222 samples.*

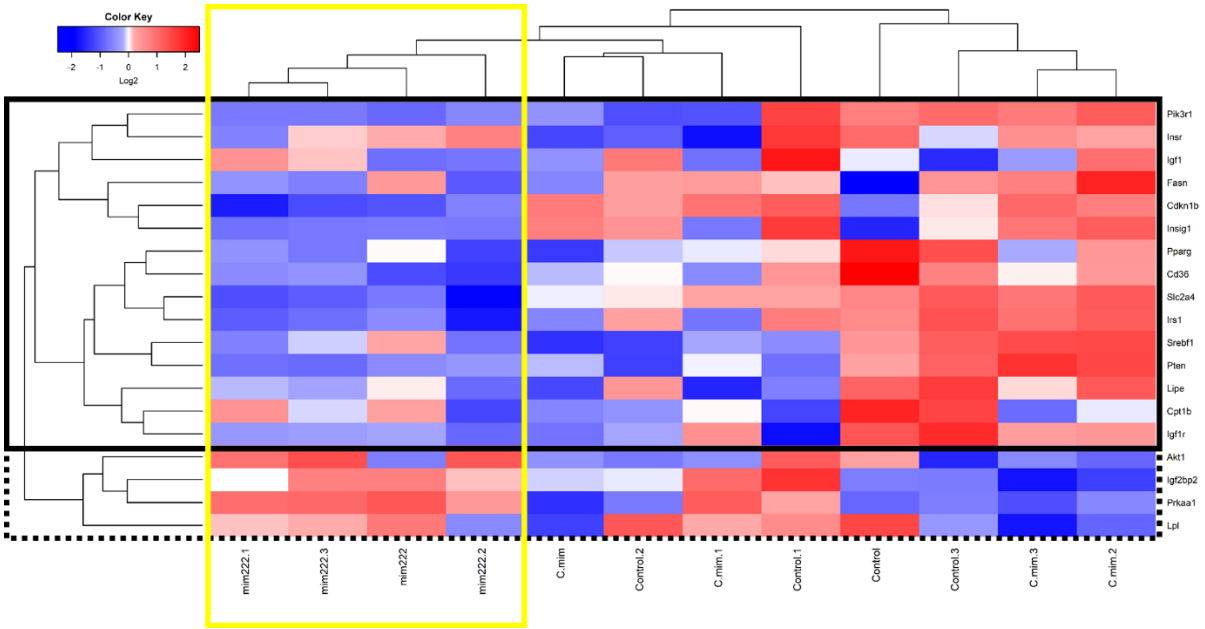

Figure 10. *Heatmap representation of microarray results for genes of interest from mature adipocytes samples. Clusters are represented for both samples (vertical) and genes (horizontal). Blue: repression. Red: overexpression. Black solid-line box: cluster of genes repressed with mim222 treatment. Black dotted-line box: cluster of genes overexpressed with mim222 treatment. Yellow solid-line box: cluster of mim222 samples.*

RT-qPCR

In order to further characterise the effect of miR222 on the gene expression of insulin signalling pathway genes, RT-qPCR technique of selected genes was performed. A greater number of samples was included in this analysis: Control, C-inh, inh222, C-mim and mim222 groups from both cell stages (preadipocytes and mature adipocytes).

Results from relative mRNA levels of selected genes related to insulin signalling in preadipocytes samples are shown in **Figure 11** and classified according to genes function. Overall, it can be seen that transfection process did not have an important negative impact in the expression of most genes as there are no significant differences between Control and C-mim or C-inh groups. In the case of *Igf1*, *Prkaa1* and *Fasn*, variances are found between Control and C-mim, while for *Lpl* variations in Control versus C-inh contrast are observed. However, in any case these significant differences are found in both negative controls at the same time, suggesting that it was not a homogenous effect.

Cdkn1b, a validated target gene for miR222, shows an important inhibition in mim222 compared to C-mim treated cells (p-value < 0.01 in C-mim versus mim222 Mann-Whitney U test). This proves that transfection with mim222, a mimetic of the native molecule, was effective and gives validation to the results.

All set of genes studied are altered due to experimental conditions. In most genes, this can be observed either as a decrease of mRNA levels when mim222 is present (such as the case of *Irs1*) or as an increase in case of inh222 presence (for example, with *Srebf1*). Most representative cases are *InsR* and *Lpl* that present both inhibitor and mimetic effects in combination. Quantitatively, the most drastic inhibition is the case of *Irs1*, with a p-value inferior to 0.001 for C-mim versus mim222 Mann-Whitney U test.

Altogether, this suggests that mim222 exerts a repression in the expression of these genes related to insulin signalling pathway. The only exception is “insulin signalling pathway antagonists” category, in which *Prkaa1* expression is enhanced in mir222 presence and *Pten* expression is unaltered.

In **Figure 12**, results from relative mRNA levels in mature adipocytes are presented, following the same classification as before. Similarly as mentioned earlier, transfection *per se* did not exhibit negative effects on general genes expression.

Unlike earlier cell stages, expression of most of the genes is not affected by the experimental treatment, neither by mim222 nor by inh222. Even *Cdkn1b* expression is not altered, which suggests that miR222 effects were not maintained to this cell differentiation point. Solely two genes exhibit significant changes. *Pkraa1* mRNA levels are increased in mim222 group, as in preadipocytes. *Cd36* shows an increase in expression in mature adipocytes from inh222 group. All the remaining differences caused in preadipocytes are lost in mature adipocytes.

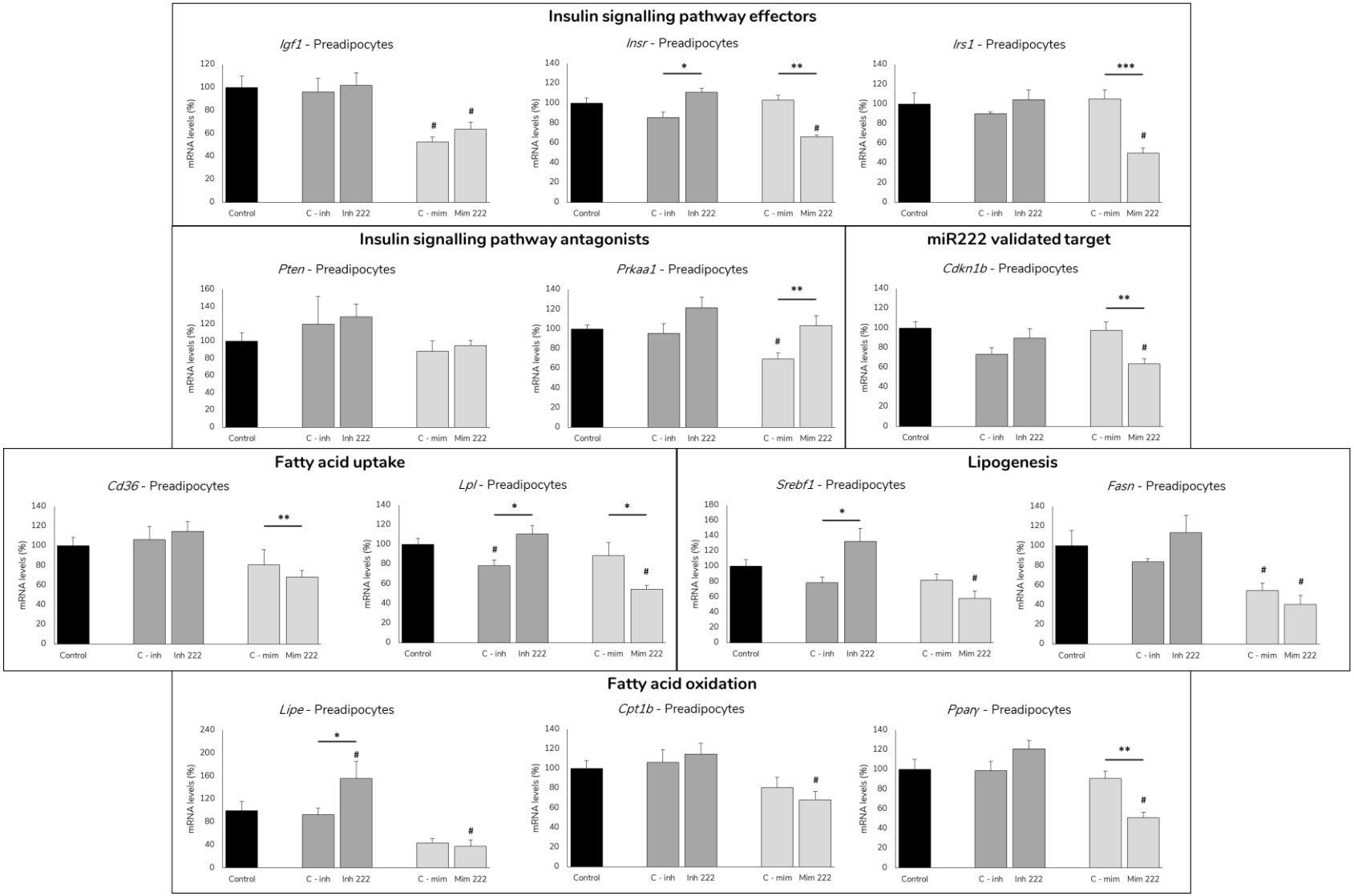

Figure 11. *Relative mRNA levels of selected genes in preadipocytes. Data are mean ± SEM. Statistics from Mann-Whitney U test: *, p<0.05; **, p<0.01; ***, p<0.001; #, p<0.05 versus Control group.*

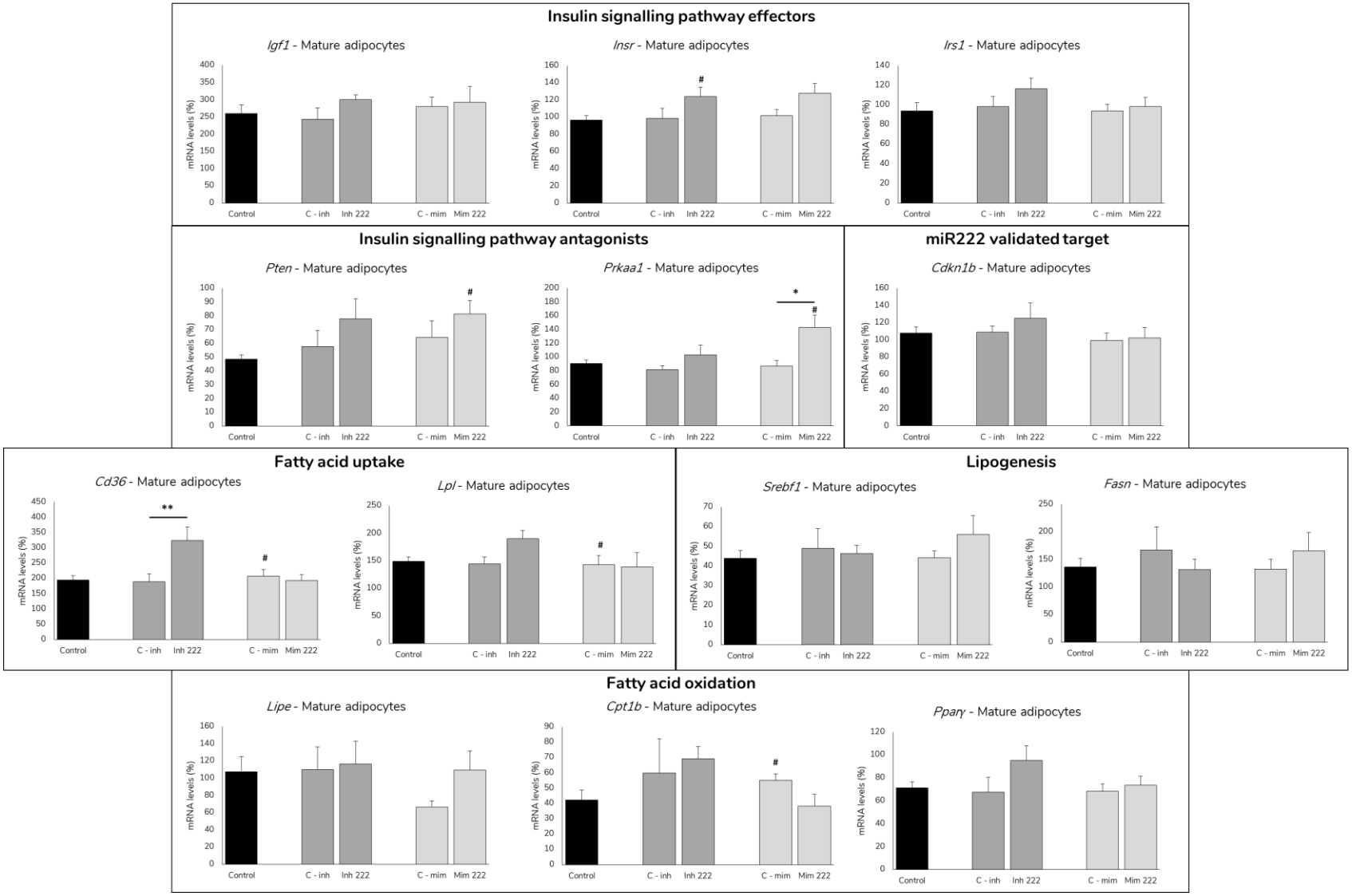

Figure 12. *Relative mRNA levels of selected genes in mature adipocytes. Data are mean ± SEM. Statistics from Mann-Whitney U test: *, p<0.05; **, p<0.01; ***, p<0.001; #, p<0.05 versus Control group.*

Validation of microarray results

To validate microarray results, analysis of selected genes by RT-qPCR was planned. This latter included a larger number of samples in each group, as described previously. Due to Covid-19 alarm state situation, experimental workload was interrupted and not all RT-qPCR analysis could be performed, particularly those for which primers were designed. Therefore, for those genes (*Akt1, Igf1r, Igf2bp2, Insig1, Pik3r1, Scl2a4*) only microarray results presented in **Table 4** will be considered for results discussion.

From this set of genes, just *Insig1* and *Igf2bp2* show a decrease in their expression, and both solely in preadipocytes. The latter presents a drastic repression, with an adjusted p-value lower than 0.001 (moderated t-test). This coincides with *in silico* analysis, which sets this gene as a target of miR222 action. No differences between mim222 and C-mim were observed in the expression of *Akt1*, *Igf1r*, *Pik3r1* and *Scl2a4*.

Table 4. *Comparison of statistical tests from the contrast C-mim versus mim222 between data from RT-qPCR and data from Microarray. Both cell stages and all genes selected are presented. ↓ : repression. ↑ : overexpression. - : no significant changes. For RT-qPCR, p-value from Mann-Whitney U was used, while for Microarray data adjusted p-value was obtained from moderated t-test. For both of them, number of arrows indicate p-value: one, p<0.05; two, p<0.01; three, p<0.001.*

Gene ID	Preadipocytes		Mature adipocytes	
	RT-qPCR	Microarray	RT-qPCR	Microarray
Akt1		-		-
Cd36	↓ ↓	↓	-	-
Cdkn1b	↓ ↓	-	-	↓
Cpt1b	-	-	-	-
Fasn	-	-	-	-
Lipe	-	-	-	-
Igf1	-	-	-	-
Igf1r		-		-
Igf2bp2		↓ ↓ ↓		-
Insig1		↓		-
Insr	↓ ↓	-	-	-
Irs1	↓ ↓ ↓	↓ ↓	-	-
Lpl	↓	-	-	-
Pik3r1		-		-
Pparγ	↓ ↓	-	-	-
Prkaa1	↑ ↑	↑	↑	-
Pten	-	↓	-	-
Scl2a4		-		-
Srebf1	-	-	-	-

In general, RT-qPCR validated microarray results. Genes that stand out in this comparison are *Cd36* and *Irs1*. They are significantly repressed in both analysis in preadipocytes stage, while in mature adipocytes no changes are observed. Therefore, they exhibit the same tendency. Another interesting gene is *Prkaa1*. Both RT-qPCR and microarray results, showed that *Pkraa1* expression was increased in preadipocytes mim222 group. This rise was also observed in mature adipocytes, but only in RT-qPCR. This could indicate that mim222 upregulated this expression of this gene.

It should also be noted that most genes that were not altered in microarray analysis displayed the same result on RT-qPCR technique. Another similarity is observed when focusing on mature adipocytes. In this cell stage, the vast majority of genes expression did not differ in C-mim versus mim222 contrast in both methods.

Other genes also show discrepancies when comparing both methods: *Cdkn1b* (in both pre- and mature adipocytes), *Insr, Lpl*, *Pparγ* and *Pten* (in preadipocytes). This could be a consequence of statistical parameters difference: for microarray, four samples were used, while for RT-qPCR a minimum of seven samples per group were included (**Table 1**). Thus, results obtained with the latter technique may be more statistically robust.

Effects of mim222 on INSR, AKT and PTEN protein levels

INSR, AKT and PTEN protein levels were studied in preadipocytes (Control, C-inh, inh222, C-mim and mim222 groups) and mature adipocytes (Control, C-mim and mim222 groups). B-ACTIN expression was used as housekeeping. Because of Covid-19 exceptional situation, protein expression analysis could not be conducted completely. AMPK1a (codified by *Prkaa1* gene) or further proteins could not be analysed. In the case of preadipocytes INSR, solely one gel electrophoresis could be done out of the three required. This diminishes the initial number of samples for this protein (**Table 1**) to 6 Control, 3 C-mim, 3 mim222, 2 C-inh and 3 inh222. Despite this, results are shown to allow further comparisons.

Preadipocytes results (**Figure 13**) show no significant differences between groups in protein levels of AKT and PTEN. For INSR, C-inh group showed a lower relative expression when compared to Control group, but previously mentioned statistical issues should be taken into consideration. In any case, this would mean transfection itself caused a repression effect in this protein expression rather than mim222. Thus, overall, it could be concluded that selected protein expression was not altered with experimental treatment.

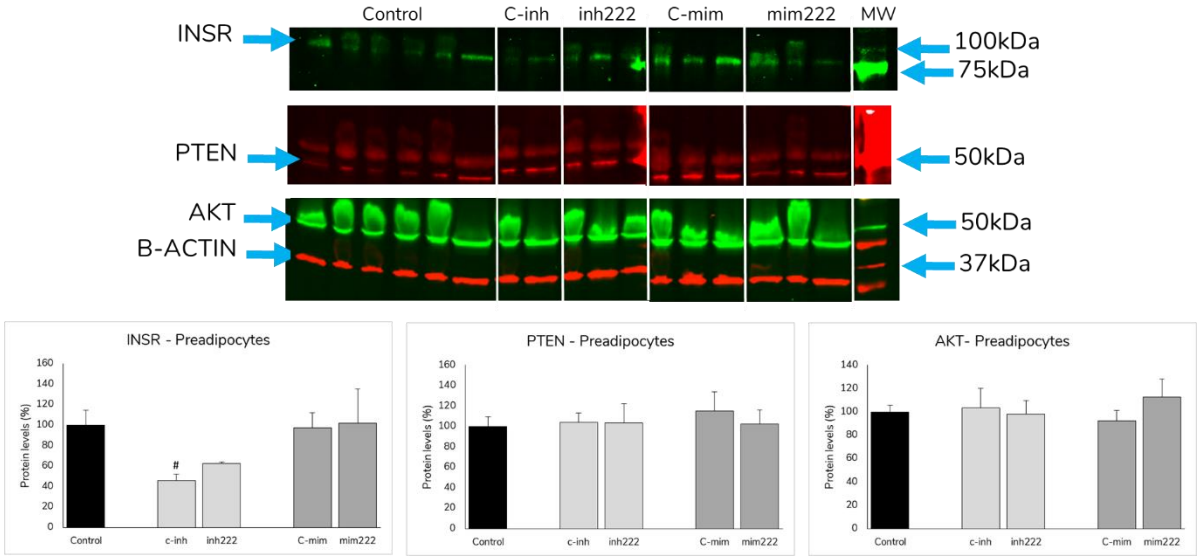

Figure 13. *Western Blotting results for preadipocytes samples. Top: membrane scans of different gels. Experimental groups shown on top. Protein identification of bands on the left. MW: molecular weight ladder. Identification of MW bands on the right. Bottom: quantification of relative protein levels corrected with B-ACTIN levels. Data are mean ± SEM. Statistics from Mann-Whitney U test: *, p<0.05; **, p<0.01; ***, p<0.001; #, p<0.05 versus Control group.*

For mature adipocytes (**Figure 14**, top), general protein expression was superior to preadipocytes: bands were more intense and better defined. Looking at scans obtained, it can be seen that mim222 group shows thinner or weaker bands when compared to C-mim in all studied proteins. This would mean that the expression of those proteins was decreased in the presence of mim222. However, at first instance, when quantitative analysis was performed, this tendency was not observed for AKT and INSR – rather than a decrease, an upregulation in mim222 group was obtained. As this did not match with photographs, calculations were repeated without standardising with B-ACTIN. After this modification, quantification results obtained were consistent with visual tendency observed in membrane scans. Therefore, a housekeeping bias was confirmed. These new results are the ones presented and discussed (**Figure 14**, bottom).

Quantification results show that, in general, mim222 group exhibits lower levels of selected proteins compared to C-mim samples. Nevertheless, only in AKT and PTEN this differences are statistically significant.

Altogether, protein expression results do not coincide with mRNA levels previously shown. In preadipocytes, *Pten* did diminish in microarray analysis but not in RT-qPCR, *Insr* decreased with mim222 treatment in RT-qPCR, whilst both *Akt* levels remained constant. All three proteins showed the same relative protein levels independently of treatment. In mature adipocytes, no difference was found between groups in either gene, while AKT and PTEN proteins show a significant decrease. This denotes variations between different layers of genetic expression: mRNA levels are not equivalent to protein expression.

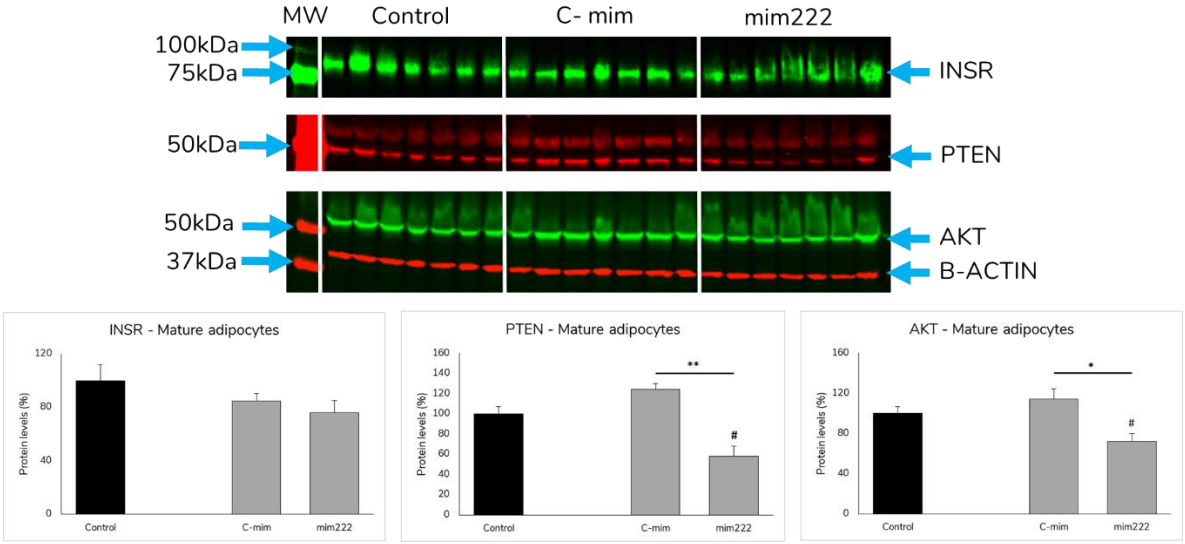

Figure 14. *Western Blotting results for mature adipocytes samples. Top: membrane scans of different gels. Experimental groups shown on top. Protein identification of bands on the right. MW: molecular weight ladder. Identification of MW bands on the left. Bottom: quantification of relative protein levels not corrected by B-ACTIN. Data are mean ± SEM. Statistics from Mann-Whitney U test: *, p<0.05; **, p<0.01; ***, p<0.001; #, p<0.05 versus Control group.*

Discussion

Previous studies show that miR222 levels are raised in obesity and metabolic syndrome and suggest that it could affect the insulin signalling pathway (10,13–17). Furthermore, this microRNA is increased in milk in dams fed a high-fat high-sucrose diet (cafeteria diet) during lactation, a situation that performs a metabolic programming on offspring (22). Thus, the scope of the present study was to determine the specific impact of miR222 on the insulin signalling pathway and confirm if it was able to exert a metabolic programming effect. To achieve this, transfection of mimetic and inhibitor molecules was performed on 3T3-L1 cell line model. Both preadipocytes and mature adipocytes cell stages were considered. Further analysis of mRNA and protein levels were conducted in order to observe significant changes. Main results suggest that the insulin signalling pathway is importantly altered with mim222 treatment and that these changes are poorly maintained until cell differentiation is complete.

To begin with, screening of signalling routes performed with microarray data shows that insulin pathway as a whole is inhibited in both preadipocytes and mature adipocytes. When studying only selected genes from the same technique, the same trend is observed (**Figure 8**). Therefore, it can be deducted that miR222 exhibits an action in the regulation of this pathway.

Metabolic programming can be defined as a process whereby a stimulus or insult at a critical period of development has lasting or lifelong significance in metabolism (26). In this study, this phenomenon was intended to be studied through different cell stages: preadipocytes, after 2 days with mim222 presence, and mature adipocytes, after 6 days without treatment (**Figure 3**). In this way, it could be seen if changes due to mim222 transfection at initial days of differentiation were conserved in mature adipocytes.

The long-term effect of mim222 treatment can be observed in the microarray experiment as three pathways related to insulin that show differences in preadipocytes are also altered in mature adipocytes. This is also true for selected genes: same mim222 repression pattern is observed in both cell stages (**Figure 9 and Figure 10**). Nonetheless, when statistical analyses are performed with microarray data, most genes with altered levels in preadipocytes are not significantly changed in mature adipocytes. Same outcomes are obtained with RT-qPCR method (**Table 4**). Only two genes (*Pkraa* and *Cd36*) out of 10 initial genes whose expression was altered with experimental conditions in the early cell stage show significant differences in mature adipocytes (**Figure 12**). Taken together, this suggests that mim222 effect is kept during differentiation process, although it gets weaker over time. In this way, after 6 days without treatment, most mRNA levels have partially recovered from inhibition and show no significant differences.

Protein results show no significant differences with mim222 treatment in preadipocytes (**Figure 13**), while for mature adipocytes an inhibition in PTEN and AKT levels is observed (**Figure 14**). These results are not congruent with previous mRNA levels, suggesting that transcription and translation regulation are not equivalent. Two possible hypothesis could explain this. On one hand, microRNAs can act through two mechanisms: enhancing mRNA degradation, which would decrease mRNA levels and therefore protein levels as well as a consequence; or preventing translation, which would only diminish protein concentration (9). It could be hypothesised that the same mim222 acted differently in distinct transcripts, thus explaining why *Akt1* is not inhibited in neither cell stage but AKT levels are significantly inferior in mature adipocytes. However, in non-embryonic cells, such as the case, mRNA decay is the dominant miRNA effect (9,27), disdaining this suggestion. On the other hand, this delay could be

explained because of different rates of transcription and translation. In fact, it has been proved that in 3T3 fibroblasts there is a significant time lap between mRNA decay and protein levels decrease after miRNA induction. Moreover, this difference was greater in the case of proteins with superior half-life, such as 100 h (27). In fact, this is the case of PTEN, which in 3T3 fibroblasts it presents approximately 132 h of half-life, much superior than mRNA half-life, around 12 h (28). Thus, in mature adipocytes, mRNA levels could have been re-established, as cells were 6 days without mim222 exposure, while protein expression did not have time to recover. It could be expected that, following the same trend as mRNA, protein would return to initial concentrations in the future.

To summarize, experiments performed support the idea that global effects of mim222 are long-lasting but not permanent. After mim222 removal, impact is especially relevant at protein level. Further experiments should be conducted to confirm if this protein effect could last any longer than the period here established. Therefore, it is suggested that miR222 cannot exert metabolic programming, at least in this *in vitro* approach. Nevertheless, several aspects need to be addressed before translating these conclusions *in vivo*. mim222 was applied in a single dose and removed after two days. However, lactation is a longer period. In rats, it lasts between 21 and 24 days, while in mice, it lasts around 21 days (29). In humans, breastfeeding is recommended to endure 6 months but can be extended up to 2 years (30). Some miRNA levels, including miR222, are increased as lactation period progresses in rats fed with a cafeteria diet (22). Moreover, it has been seen that microRNAs are stable in body fluids: "they are protected from degradation by RNAses because they are contained in small membranous vesicles, packaged within HDLs and linked to RNA-binding proteins" (17). Thus, exposition to miR222 during lactation can reach much greater levels than here emulated. In consequence, it could be possible that physiological miR222 impact was of such a magnitude that it could exert a metabolic programming.

As mentioned before, miR222 is believed to play a role in IR in obesity. Proteins are the effectors of cell function. Therefore, it could be expected to argue potential physiological effects of miR222 based on these molecules. "Despite the ultimate importance of the protein changes, measuring these changes over time is less informative for analysing miRNA repression dynamics than is measuring mRNA changes, which more directly captures the molecular effects of the miRNA in inhibiting translation and destabilizing mRNA" (27). Considering this, special attention will be paid to genes of interest that show a greater change in mRNA analysis, as these variations could have an important impact on IR onset: *Insr, Irs1, Lpl, Cd36, Prkaa* and *Igf2bp2*.

Insr mRNA levels are decreased in mim222 compared to C-mim and increased in inh222 compared to C-inh in preadipocytes (**Figure 11**). This effect is partially observed at protein level in mature adipocytes: INSR expression is slightly lower in mim222 when compared to C-mim, without reaching statistical significance (**Figure 14**). Even though it could be thought that *Insr* is a miR222 target gene, no theoretical matches are found in miRDB searches (24). Therefore, it could be an indirect repression effect. INSR is the first effector of insulin signalling pathway (**Figure 1**). Consequently, it seems obvious to think that a lower expression of this receptor will have negative repercussions in insulin signalling. This was demonstrated in a mouse model with a fat-specific knockout of INSR. The null presence of INSR in adipocytes caused a marked IR, among other symptoms of lipodystrophy (31). On the contrary, it was seen that overexpression of INSR in a genetic model of obesity (db/db) partially improved obese and diabetic phenotypes (32). In addition, a human "normal cell contains around 20.000 INSR on surface, while an insulin resistant cell presents only about a quarter of the number of receptor sites to

that in a normal cell" (33). Overall, it can be assumed that diminished expression of INSR is linked to IR, and therefore miR222 could contribute to this phenotype in this way.

In preadipocytes, *Irs1* mRNA levels show the most drastic decrease in mim222 compared to C-mim, reaching 50 % inhibition (**Figure 11**). These results agree with previous studies. In concrete, it was seen that miR222 was increased in liver of high fat/high sucrose diet fed mice and it repressed IRS1 expression. It was also confirmed that both human and mouse *Irs1* genes are direct targets of miR222 (20). The present work suggests that this repression can be extended to adipose tissue. Several works associate IRS1 repression with insulin resistance or/and T2D. An *Irs1* knockout mouse model exhibited mild insulin resistance (34). In a human hepatocellular carcinoma cell line (HepG2 cells) with induced IR, a compound ameliorate their phenotype via increase of IRS1 levels (35). Finally, in humans, several mutations on this gene have been associated with T2D (36–38) and gestational diabetes (39), emphasising the importance of this protein on this pathology onset. Consequently, miR222 repression effect on *Irs1* could be related to impaired insulin sensitivity.

Fatty acid uptake function in preadipocytes is affected by experimental treatment. Differences are found in mim222 vs C-mim and inh222 vs C-inh contrasts for *Lpl* and in mim222 vs C-mim comparison for *Cd36* (**Figure 11**). The latter is also observed in mature adipocytes (**Figure 12**), being one of the few long-term conserved effects. Therefore, miR222 has an impact on both genes expression.

LPL is the rate-limiting enzyme for the hydrolysis of the triglyceride (TG) core of circulating lipoproteins (40). In adipose tissue, insulin increases *Lpl* mRNA levels by increasing gene transcription (41). Thus, down-regulation here showed could be consequence of the insulin route impairment rather than a direct miR222 effect. It is well known that LPL deficiency is the main cause of chylomicronemia syndrome, characterised by elevated triglycerides (42). However, when this enzyme is absent exclusively in adipose tissue, as recreated in a mouse transgenic model, no significant changes are seen in body weight or body composition (43). Consequently, no direct relation between the repression here seen and obesity phenotype can be established.

Cd36 is a scavenger receptor important for fatty acid uptake and release in response to lipolytic stimuli in adipose tissue (44). It was observed in a spontaneously hypertensive rat model which presented IR that CD36 expression was deficient. When transgenic mice overexpressing this receptor were generated, IR phenotype improved (45). In humans, this is also true as genetic CD36 deficiency is associated with IR and abnormal fatty acid metabolism (46) and variants of the gene are associated with either metabolic syndrome or T2D (47,48). Therefore, miR222 impact on *Cd36* expression could have a significant effect on obesity related complications onset.

Pkraa has higher mRNA levels in mim222 group compared to C-mim in both preadipocytes and mature adipocytes (**Figure 11 and Figure 12**), being, besides *Cd36*, the only gene that shows maintained effects. *Pkraa* codifies for AMPK. AMPK is activated in energy stress and has effects to reduce ATP consumption and to enhance ATP production. The former is achieved by inhibition of biosynthesis pathways, such as protein translation, supressing TSC2; or lipogenesis, supressing acetyl-CoA carboxylases activity. The latter is enhanced through stimulation of glucose uptake (through GLUT4, among others), glucose and lipids usage and autophagy (49). Hence, AMPK activation stimulus are contrary to insulin signalling pathway ones, and most of their downstream effects are opposed. However, as AMPK also improves mitochondrial function and inhibits inflammation, which are involved in IR onset, its activation improves insulins sensitivity. Many studies demonstrate that AMPK down-

regulation triggers IR. Lower activity of AMPK was found in adipose tissue of both animal models for metabolic syndrome/obesity and in humans with Cushing's syndrome (which is characterized by IR). Moreover, some antidiabetic drugs act as AMPK activators, such as metformin (50). Considering this, the upregulation of AMPK caused by miR222 would contribute to ameliorate IR panorama, contrasting previous effects described.

Igf2bp2 was a predicted target gene of miR222. Data obtained validates this, as mRNA levels were significantly lower in mim222 compared to C-mim in preadipocytes (**Table 4**). It was seen that IGF2BP2 can activate PI3K/AKT signalling pathway in pancreatic cancer cells (51). Thus, decreased expression of this protein mediated by miR222 could inhibit insulin signalling pathway and enhance IR-related clinical complications. In fact, in humans several variants of *Igf2bp2* gene have been related to T2D (52,53).

These many repression effects did not have an appreciable impact neither on morphological cell aspects (**Figure 5**) nor on cellular lipid content (**Figure 7**). The latter was decreased in mim222 compared to C-mim, even though the difference was not statistically significant. This could be explained by the increase in *Pkraa* and the decrease in both *Lpl* and *Cd36*. Fatty acid uptake would be decreased while catabolism would be stimulated. Besides, as insulin signalling pathway stimulates lipogenesis and it would be repressed, fewer lipids would be generated. As explained before, most changes were not maintained until mature adipocytes, reason why this reduction in lipid content may have been restored to initial situation, erasing significant differences.

Overall, the present study suggests that miR222 represses many effectors of insulin signalling pathway in 3T3-L1 adipocytes. Previous studies performed in the same cell line model already showed inhibition effects on important proteins for IR development, such as GLUT4 (18) and AdipoR1 (19). Taken together, it is suggested that this microRNA might partly explain the link between obesity and IR – obesity rises miR222 levels, which would in turn supress insulin signalling route. IR would be developed in consequence, leading to further complications such as T2D. This offers an additional explanation to current elucidated IR mechanisms, which mainly include post-transcriptional modifications of pathway effectors (6). It should also be noted that miR222 would not act alone – this impact could be complemented with other microRNAs altered in obesity and that could also affect this pathway, such as miR26a, miR200, miR29, miR130 or let-7 (10,22).

Conclusions

- mim222 transfection in 3T3-L1 cell line correctly emulated miR222 effect, as validated target genes (*Cdkn1b, Irs1*) expression was diminished
- miR222 has an overall repressing effect on insulin signalling pathway
- Down-regulation of insulin route effectors caused by miR222, such as *InsR, Irs1* or *Cd36,* could be linked to insulin resistance observed in obesity
- *In vitro* approach could not confirm miR222 metabolic programming effects – impact was long-lasting but not permanent

References

1. World Health Organization (WHO). Obesity and overweight [Internet]. 2020 [cited 2020 May 6]. Available from: https://www.who.int/en/news-room/fact-sheets/detail/obesity-and-overweight

2. Spiegelman BM, Flier JS. Obesity and the regulation of energy balance. Vol. 104, Cell. Cell Press; 2001. p. 531–43.

3. Desai M, Jellyman JK, Ross MG. Epigenomics, gestational programming and risk of metabolic syndrome. Int J Obes. 2015 Apr 9;39(4):633–41.

4. Kalupahana NS, Moustaid-Moussa N, Claycombe KJ. Immunity as a link between obesity and insulin resistance. Mol Aspects Med. 2012;33(1):26–34.

5. Alberti KGMM, Zimmet P, Shaw J. The metabolic syndrome - A new worldwide definition. Lancet. 2005;366(9491):1059–62.

6. Gutiérrez-Rodelo C, Roura-Guiberna Jesús Alberto Olivares-Reyes A, Alberto Olivares-Reyes J. Mecanismos Moleculares de la Resistencia a la Insulina: Una Actualización. Gac Med Mex. 2017;153:214–42.

7. Haeusler RA, McGraw TE, Accili D. Biochemical and cellular properties of insulin receptor signalling. Nat Rev Mol Cell Biol. 2018 Jan;19(1):31–44.

8. Singh P, Alex JM, Bast F. Insulin receptor (IR) and insulin-like growth factor receptor 1 (IGF-1R) signaling systems: novel treatment strategies for cancer. Med Oncol. 2014 Jan 14;31(1):805.

9. Bartel DP. Metazoan MicroRNAs. Cell. 2018 Mar 22;173(1):20–51.

10. Deiuliis JA. MicroRNAs as regulators of metabolic disease: pathophysiologic significance and emerging role as biomarkers and therapeutics. Int J Obes. 2016 Jan;40(1):88–101.

11. Wang Y, Liang Y, Lu Q. MicroRNA epigenetic alterations: Predicting biomarkers and therapeutic targets in human diseases. Clin Genet. 2008;74(4):307–15.

12. Li Y, Kowdley K V. MicroRNAs in Common Human Diseases. Genomics, Proteomics Bioinforma. 2012;10(5):246–53.

13. Ortega FJ, Mercader JM, Catalán V, Moreno-Navarrete JM, Pueyo N, Sabater M, et al. Targeting the circulating microRNA signature of obesity. Clin Chem. 2013 May 1;59(5):781–92.

14. Chartoumpekis D V, Zaravinos A, Ziros PG, Iskrenova RP, Psyrogiannis AI. Differential Expression of MicroRNAs in Adipose Tissue after Long-Term High-Fat Diet-Induced Obesity in Mice. PLoS One. 2012;7(4):34872.

15. Herrera BM, Lockstone HE, Taylor JM, Ria M, Barrett A, Collins S, et al. Global microRNA expression profiles in insulin target tissues in a spontaneous rat model of type 2 diabetes. Diabetologia. 2010;53:1099–109.

16. Cui X, You L, Zhu L, Wang X, Zhou Y, Li Y, et al. Change in circulating microRNA profile of obese children indicates future risk of adult diabetes. Metabolism. 2018;78:95–105.

17. Manuel J, Fern´fernández-Real F, Ortega FJ, Mercader JM, María Moreno-Navarrete J, Rovira O, et al. Profiling of Circulating MicroRNAs Reveals Common MicroRNAs Linked to Type 2 Diabetes That Change With Insulin Sensitization. Diabetes Care. 2014;37:1375–83.

18. Shi Z, Zhao C, Guo X, Ding H, Cui Y, Shen R, et al. Differential Expression of MicroRNAs in Omental Adipose Tissue From Gestational Diabetes Mellitus Subjects Reveals miR-222 as a Regulator of ERα Expression in Estrogen-Induced Insulin Resistance. Endocrinology. 2014 May 1;155(5):1982–90.

19. Gan M, Shen L, Wang S, Guo Z, Zheng T, Tan Y, et al. Genistein inhibits high fat diet-induced obesity through miR-222 by targeting BTG2 and adipor1. Food Funct. 2020;11:2418.

20. Ono K, Igata M, Kondo T, Kitano S, Takaki Y, Hanatani S, et al. Identification of microRNA that represses IRS-1 expression in liver. PLoS One. 2018;13(1):e0191553.

21. Li B, Lu Y, Yu L, Han X, Wang H, Mao J, et al. miR-221/222 promote cancer stem-like cell properties and tumor growth of breast cancer via targeting PTEN and sustained Akt/NF-κB/COX-2 activation. Chem Biol Interact. 2017 Nov 1;277:33–42.

22. Pomar CA, Castro H, Picó C, Serra F, Palou A, Sánchez J. Cafeteria Diet Consumption during Lactation in Rats, Rather than Obesity Per Se, alters miR-222, miR-200a, and miR-26a Levels in Milk. Mol Nutr Food Res. 2019 Apr;63(8):1800928.

23. Insulin Signaling (Mus musculus) - WikiPathways [Internet]. [cited 2020 May 8]. Available from: https://www.wikipathways.org/index.php/Pathway:WP65

24. Chen Y, Wang X. miRDB: an online database for prediction of functional microRNA targets. Nucleic Acids Res. 2019;48:127–31.

25. Yang Y-F, Wang F, Xiao J-J, Song Y, Zhao Y-Y, Cao Y, et al. MiR-222 overexpression promotes proliferation of human hepatocellular carcinoma HepG2 cells by downregulating p27. Int J Clin Exp Med. 2014;7(4):893.

26. Lucas A. Programming by early nutrition in man. Ciba Found Symp. 1991;156:35–8.

27. Eichhorn SW, Guo H, McGeary SE, Rodriguez-Mias RA, Shin C, Baek D, et al. MRNA Destabilization Is the dominant effect of mammalian microRNAs by the time substantial repression ensues. Mol Cell. 2014 Oct 2;56(1):104–15.

28. Schwanhüusser B, Busse D, Li N, Dittmar G, Schuchhardt J, Wolf J, et al. Global quantification of mammalian gene expression control. Nature. 2011 May 19;473(7347):337–42.

29. Gullace F. Reproducción de los animales de laboratorio. In: Fisiologia veterinaria. McGraw-Hill Interamericana; 1995. p. 987–98.

30. World Health Organization (WHO). Infant and young child feeding [Internet]. [cited 2020 Jun 19]. Available from: https://www.who.int/en/news-room/fact-sheets/detail/infant-and-young-child-feeding

31. Softic S, Boucher J, Solheim MH, Fujisaka S, Haering M-F, Homan EP, et al. Lipodystrophy Due to Adipose Tissue-Specific Insulin Receptor Knockout Results in Progressive NAFLD. Diabetes. 2016;65:2187–200.

32. Sasaki T, Kuroko M, Sekine S, Matsui S, Kikuchi O, Susanti VY, et al. Overexpression of insulin receptor partially improves obese and diabetic phenotypes in db/db mice. Endocr J. 2015 Sep 30;62(9):787–96.

33. Hanas R. Type 2 Diabetes in Adults of All Ages. Class Publishing; 2007.

34. Tang CY, Man XF, Guo Y, Tang HN, Tang J, Zhou C La, et al. IRS-2 partially compensates for the insulin signal defects in IRS-1–/– mice mediated by miR-33. Mol Cells. 2017 Feb 1;40(2):123–32.

35. Xuguang H, Aofei T, Tao L, Longyan Z, Weijian B, Jiao G. Hesperidin ameliorates insulin resistance by regulating the IRS1-GLUT2 pathway via TLR4 in HepG2 cells. Phyther Res. 2019 Jun 1;33(6):1697–705.

36. Albegali AA, Shahzad M, Mahmood S, Ullah MI. Genetic association of insulin receptor substrate-1 (IRS-1, rs1801278) gene with insulin resistant of type 2 diabetes mellitus in a Pakistani population. Mol Biol Rep. 2019 Dec 1;46(6):6065–70.

37. Alharbi KK, Khan IA, Munshi A, Alharbi FK, Al-Sheikh Y, Alnbaheen MS. Association of the genetic variants of insulin receptor substrate 1 (IRS-1) with type 2 diabetes mellitus in a Saudi population. Endocrine. 2014 Oct 21;47(2):472–7.

38. Shakeri H, Khoshi A, Kaffash Bajestani M, Farahi A, Javadzadeh MS, Hosseini Z, et al. Association of IRS1 Gly971arg gene polymorphism with insulin resistance in Iranian newly diagnosed diabetic adults. Acta Endocrinol (Copenh). 2019 Jul 1;15(3):317–22.

39. KK A, IA K, Z A, MM A-H. Insulin Receptor substrate-1 (IRS-1) Gly927Arg: Correlation With Gestational Diabetes Mellitus in Saudi Women. Biomed Res Int. 2014;2014.

40. Wang H, Eckel RH. Lipoprotein lipase: From gene to obesity. Vol. 297, American Journal of Physiology - Endocrinology and Metabolism. American Physiological Society; 2009.

41. Semenkovichs CF, Wimss M, Noes L, Etienneq J, Chans L. Insulin Regulation of Lipoprotein Lipase Activity in 3T3-Ll Adipocytes Is Mediated at Posttranscriptional and Posttranslational Levels. J Biol Chem. 1989;264(15):9030–8.

42. Falko JM. Familial chylomicronemia syndrome: A clinical guide for endocrinologists. Vol. 24, Endocrine Practice. American Association of Clinical Endocrinologists; 2018. p. 758–63.

43. Weinstock PH, Levak-Frank S, Hudgins LC, Radner H, Friedman JM, Zechner R, et al. Lipoprotein lipase controls fatty acid entry into adipose tissue, but fat mass is preserved by endogenous synthesis in mice deficient in adipose tissue lipoprotein lipase. Proc Natl Acad Sci U S A. 1997 Sep 16;94(19):10261–6.

44. Pietka TA, Schappe T, Conte C, Fabbrini E, Patterson BW, Klein S, et al. Adipose and muscle tissue profile of CD36 transcripts in obese subjects highlights the role of CD36 in fatty acid homeostasis and insulin resistance. Diabetes Care. 2014;37(7):1990–7.

45. Aitman TJ, Glazier AM, Wallace CA, Cooper LD, Norsworthy PJ, Wahid FN, et al. Identification of Cd36 (Fat) as an insulin-resistance gene causing defective fatty acid and glucose metabolism in hypertensive rats. Nat Genet. 1999 Jan;21(1):76–83.

46. Kuwasako T, Hirano KI, Sakai N, Ishigami M, Hiraoka H, Yakub MJ, et al. Lipoprotein abnormalities in human genetic CD36 deficiency associated with insulin resistance and abnormal fatty acid metabolism. Diabetes Care. 2003 May 1;26(5):1647–8.

47. Love-Gregory L, Sherva R, Sun L, Wasson J, Schappe T, Doria A, et al. Variants in the CD36 gene associate with the metabolic syndrome and high-density lipoprotein cholesterol. Hum Mol Genet. 2008;17(11):1695–704.

48. Corpeleijn E, Van Der Kallen CJH, Kruijshoop M, Magagnin MGP, De Bruin TWA, Feskens EJM, et al. Direct association of a promoter polymorphism in the CD36/FAT fatty acid transporter gene with type 2 diabetes mellitus and insulin resistance. Diabet Med. 2006 Aug;23(8):907–11.

49. Herzig S, Shaw RJ. AMPK: guardian of metabolism and mitochondrial homeostasis. Nat Rev Mol Cell Biol. 2018;19(2):121–35.

50. Neil B. Ruderman, David Carling, Marc Prentki, José M. Cacicedo. AMPK, insulin resistance, and the metabolic syndrome. J Clin Invest. 2013 Jul;123(7):2764–72.

51. Xu X, Yu Y, Zong K, Lv P, Gu Y. Up-regulation of IGF2BP2 by multiple mechanisms in pancreatic cancer promotes cancer proliferation by activating the PI3K/Akt signaling pathway. J Exp Clin Cancer Res. 2019 Dec 18;38(1).

52. Wu HH, Liu NJ, Yang Z, Tao XM, Du YP, Wang XC, et al. IGF2BP2 and obesity interaction analysis for type 2 diabetes mellitus in Chinese Han population. Eur J Med Res. 2014;19(1).

53. Gu T, Horová E, Möllsten A, Seman NA, Falhammar H, Prázný M, et al. IGF2BP2 and IGF2 genetic effects in diabetes and diabetic nephropathy. J Diabetes Complications. 2012 Sep;26(5):393–8.